

## RESEARCH ARTICLE

# ADD-Net: An Effective Deep Learning Model for Early Detection of Alzheimer Disease in MRI Scans

MIAN MUHAMMAD SADIQ FAREED<sup>1</sup>, SHAHID ZIKRIA<sup>2</sup>, GULNAZ AHMED<sup>1</sup>, MUI-ZZUD-DIN<sup>3</sup>, SAQIB MAHMOOD<sup>4</sup>, MUHAMMAD ASLAM<sup>5</sup>, SYEDA FIZZAH JILLANI<sup>6</sup>, AHMAD MOUSTAFA<sup>7</sup>, AND MUHAMMAD ASAD<sup>8</sup>, (Student Member, IEEE)

<sup>1</sup>Institute of Artificial Intelligence and Marine Robots, Dalian Maritime University, Dalian 116026, China

<sup>2</sup>Department of Computer Science, Information Technology University, Lahore 54000, Pakistan

<sup>3</sup>Department of Computer Science, Ghazi University, Dera Ghazi Khan 32200, Pakistan

<sup>4</sup>Department of Computer Science, Khwaja Fareed University of Engineering and Information Technology, Rahim Yar Khan 64200, Pakistan

<sup>5</sup>School of Computing Engineering and Physical Sciences, University of the West of Scotland, Glasgow G72 0LH, U.K.

<sup>6</sup>Department of Physics, Physical Sciences Building, Aberystwyth University, Aberystwyth SY23 3FL, U.K.

<sup>7</sup>Department of Computer Science, Nagoya Institute of Technology, Nagoya 466-0061, Japan

<sup>8</sup>Graduate School of Information Science and Technology, The University of Tokyo, Tokyo 113-8654, Japan

Corresponding authors: Gulnaz Ahmed (gulnaz@xjtu.edu.cn) and Muhammad Aslam (muhammad.aslam@uws.ac.uk)

**ABSTRACT** Alzheimer's Disease (AD) is a neurological brain disorder marked by dementia and neurological dysfunction that affects memory, behavioral patterns, and reasoning. Alzheimer's disease is an incurable disease that primarily affects people over 40. Alzheimer's disease is diagnosed through a manual evaluation of a patient's MRI scan and neuro-psychological examinations. Deep Learning (DL), a type of Artificial Intelligence (AI), has pioneered new approaches to automate medical image diagnosis. This study aims to create a reliable and efficient system for classifying AD using MRI by applying the deep Convolutional Neural Network (CNN). In this paper, we propose a new CNN architecture for detecting AD with relatively few parameters, and the proposed solution is ideal for training a smaller dataset. This proposed model successfully distinguishes the early stages of Alzheimer's disease and shows class activation maps as a heat map on the brain. The proposed Alzheimer's Disease Detection Network (ADD-Net) is built from scratch to precisely classify the stages of AD by decreasing parameters and calculation costs. The Kaggle MRI image dataset has a significant class imbalance problem, and we exploited a synthetic oversampling technique to evenly distribute the image among the classes to prevent the problem of class imbalance. The proposed ADD-Net is extensively evaluated against DenseNet169, VGG19, and InceptionResNet V2 using precision, recall, F1-score, Area Under the Curve (AUC), and loss. The ADD-Net achieved the following values for evaluation metrics: 98.63%, 99.76%, 98.61%, 98.63%, 98.58%, and 0.0549% accuracy, AUC, F1-score, precision, recall, and loss, respectively. The simulation results show that the proposed ADD-Net outperforms other state-of-the-art models in all the evaluation metrics.

**INDEX TERMS** Deep learning, image classification, supervised learning, transfer learning, imbalanced data-set, MRI data-set, computer-aided diagnosis, SMOTETOMEK, class activation.

## I. INTRODUCTION

Alzheimer's Disease (AD) is the most frequent kind of dementia that needs substantial medical attention. Early and precise analysis of AD prognosis is required to start

The associate editor coordinating the review of this manuscript and approving it for publication was Wenming Cao <sup>id</sup>.

therapeutic progress, and efficient patient therapy [1]. According to a study, 10 million new cases of dementia are registered every year [2]. The World Health Organization (WHO) reported that AD had surpassed cancer as the fifth most significant cause of death, with the number of AD patients expected to reach 152 million by 2050 [2]. AD is a long-term neurological brain disease that gradually destroys

brain cells, causing memory loss and cognitive problems and finally accelerating the loss of ability to perform day-to-day activities of real-life [3].

AD is a brain-neurological degeneration disorder [4]. It is categorized as dementia, atrophy of the human brain affecting memory, and causes loss of behavioral, social, and reasoning faculties. It is caused by the accumulation of protein fragments in the brain [5], [6], [7]. Plaques and tangles are formed around the neurons inside the human brain, which results in abnormal shrinking of lobes and hippocampus, and enlarged ventricles [8]. It is an incurable fatal disease [9], [10] with a lifetime of agony for the patient and a severe mental, physical, and financial toll of suffering for the patient's family. The cause of AD is unknown, and there are no effective medications or therapies to reverse dementia. Mild Cognitive Impairment (MCI), a pre-clinical stage of AD, is a transitory state between normal ageing and AD.

Detecting the risk and severity of AD at its early stages is very critical [11], [12]. However, Doctors can classify AD in its early stages using neuro-imaging and computer-assisted diagnostic approaches with less accuracy. Neuro-imaging, including Computed Tomography (CT) scan, Positron Emission Tomography (PET) scan, and specifically Magnetic Resonance Imaging (MRI) scan, play a vital role in medical diagnosis [4]. It is an effective non-invasive method that provides information about the human body. The advancement of the medical diagnosis process has created tremendous research trends in computer-aided diagnosis nowadays [5], [6].

Over the years, numerous Machine Learning (ML) [13] and Deep Learning (DL) [14] algorithms have been developed by many researchers around the globe for AD detection and classification. Many researchers have achieved remarkable results using the DL algorithms. However, there is still room for improvement. In this series of DL models, a hybrid Convolutional Neural Network (CNN), a CNN model with slice selection, and a CNN model with histogram stretching are introduced in [15], [16], and [17]. Others proposed a CNN model with skull striping [18] and a CNN model which utilized the slicing samples for pre-processing is introduced in [19]. However, the focus of these deep models is primarily biased towards classification due to the black-box nature of CNN.

In the literature on AD, some researchers have developed miscellaneous tools and applications for automated segmentation of neuro-images [20]. These applications are Vol-Brain [21], and Fusion of neuro-imaging Pre-processing [22]. Although these applications are practical tools for segmenting neuro-image, the research focused on visualizing the classification process through CNN layers is scarce. The feature map of each convolution layer reveals various filters being applied to the image, and it provides a hint as to what sort of filters the model uses to the image for feature extraction [23]. This approach supports grad-CAM [24] heatmap, which shows class activation via gradient-based localization map.

The proposed CNN model uses a series of conventional blocks consisting of different deep layers to accomplish outstanding classification results. The proposed ADD-Net aims to obtain an accurate classification result for detecting AD in its earlier stages with better accuracy. The main contributions of the research study are:

- We propose a new convolutional neural network architecture for detecting AD with relatively few parameters, and the proposed solution is ideal for training a smaller dataset.
- The previous methods [22], [23], [25] accuracy compromised on Alzheimer's data-set due to an imbalanced number of classes. To handle the imbalance problem of the Alzheimer's data set, we exploited the SMOTE-TOMEK oversampling algorithm, which interpolates new images to balance the class samples.
- In our proposed model, we used the Grad-CAM to show and highlight the infected part of the brain for different stages of Alzheimer's disease, and the generated heat map intensities highlight each stage's severity.
- The proposed model is extensively compared with several other approaches using various evaluation parameters: Accuracy, AUC, Precision, Recall, F1-score, and size of trainable parameters. It is observed that our approach outperforms other state-of-the-art models.

The rest of the paper is arranged in the following way: The related studies of the proposed model are briefed in section II. The methodology and proposed ADD-Net model for AD classification details are presented with the description of the dataset, and model components are shown in section III. The visualization process and the ADD-Net model evaluation with the state-of-the-art models are presented in section IV. The ADD-Net's limitations and the conclusion with future goals are described in section V and section VI, respectively.

## II. RELATED WORK

Precise classification of medical images is a strenuous task because of the complicated procedure of obtaining medical data sets [25]. Unlike other data sets, medical data sets are prepared by expert specialists and contain sensitive and private information about patients, which cannot be publicly disclosed to anyone. That is why organizations and institutions like Alzheimer's Disease Neuroimaging Initiative (ADNI) [26] and Open Access Series of Imaging Studies (OASIS) [27] providing medical data-sets have a screening process for accessing their data-sets which requires an application to be filled and terms to be agreed by the researcher, constraining them from using it for research purposes only [28], [29], [30], [31]. Medical data sets are inherently highly imbalanced because it is impossible to compile a data set with an equal number of patients with health and ailment samples. The techniques to tackle this problem are pretty challenging themselves [32], [33], [34], [35]. OASIS data-set containing 416 3D samples is used by Islam and Zhang [36] to create a CNN model with the convolution

**TABLE 1.** Literature evaluation of numerous recent cutting-edge approaches used in AD detection and classification.

Approach	Year	Method	Results					Modalities	Imbalance Handling
			Accuracy	AUC	Precision	Recall	F1-Score		
Shereen [29]	2021	DenseNet201, ResNet101	94.86%	-	89.47%	83.74%	95.36%	4	None
Badiea [30]	2021	AlexNet + SVM & AlexNet + ResNet50	94.8%	99.7%	-	-	-	2	None
Pradhan [31]	2021	DenseNet169 & VGG19	82.6%	86.7%	-	-	-	2	None
Vasukidevi [32]	2021	CapsNet	94.3%	-	94.92%	95.89%	95.19%	1	None
Battineni [33]	2021	CNN Model	83.3%	-	-	-	-	1	None
Suganthe [16]	2021	Inception-ResNet-v2	79.12%	81.9%	70.64%	28.22%	39.91%	1	None
Jyoti [34]	2018	InceptionV4 + ResNet + ADNet	93.18%	-	94%	93%	92%	5	Data Augmentation
Jyoti [35]	2017	DenseNet121 + DenseNet161 + DenseNet169	93.18%	-	94%	93%	92%	4	None
Jyoti [36]	2017	InceptionV4	73.75%	-	-	-	-	1	None

layer, batch normalization layer, pooling layer, and Adam optimizer.

To evaluate their model accuracy, the authors compared their model with two different pre-trained architectures like InceptionV4 [37] and ResNet [37]. To overcome the data-set imbalance problem, a cost-sensitive training technique is discussed in [38]. The cost matrix modified the result of the output layer to give more importance to classes with fewer samples, and the experiments achieved a precision of 75%. A comparative analysis of state-of-the-art Alzheimer's disease classification models is depicted in Table 1; we can note that the traditional deep and transfer learning models achieve good accuracy on the imbalanced datasets.

A similar approach is adopted by Khan *et al.* [38] for the same OASIS data set. They used a 12-layer CNN architecture, including convolution and pooling operations. They used Leaky ReLU [39] in combination with MaxPooling as activation function instead of ReLU [40] to avoid gradient vanishing issue [41]. The authors compared their model with four different pre-trained models like InceptionV3, Xception [42], MobileNetV2 [43], and VGG19 [25] to analyze the performance of the model. The model achieves an accuracy of 97.75% during experiments compared to pre-trained models.

The same data set from Kaggle is used by Ebrahimgahnavieh *et al.* [14] to implement a hybrid framework using ResNet V2 with Inception V4. In this model, the ResNet V2 integrates residual connections to the pre-trained Inception V4 model [38]. In the experiments, the model is assessed by varying learning rates and optimizers, producing the highest accuracy of 79.12%. Pradhan *et al.* [31] perform a simple comparative study using two state-of-the-art pre-trained models like VGG19 and DenseNet169 [44]. These two models are selected due to the ability of VGG19

to train on many classes with remarkable accuracy, and the DenseNet169 can handle vanishing gradient issues and reduce the number of training parameters. The data set from Kaggle was fed to both models via Image Data Generator (IDG) with different augmentation parameters. Through the augmentation, the pre-trained models like VGG19 and DenseNet169 achieved an accuracy of 88% and 87%, respectively. Battineni *et al.* [33] employed an OASIS-3 data set and created a five-layer CNN model to classify three different early stages of Alzheimer's disease [45].

Not all the features extracted by a deep model are helpful in accurately predicting the correct class of a sample, and some hinder a model from reaching desired results [46], [47]. This issue of deep models was tackled by El-Aal *et al.* [29] and presented a novel approach to selecting specific features from the feature map of deep models, which ultimately improves the classification results and reduces the training time of the model. The ResNet101 and DenseNet201 for feature extraction, while the Rival Genetic Algorithm (RGA) [48] and Probability Binary Particle Swarm Optimization (PBPSO) [49] algorithms were used for feature selection. The selected and control features were fed to a separately created classification model. ResNet101 and DenseNet201 provided the best results with PBPSO and achieved an accuracy of 87.3% and 94.8%, respectively. Raju *et al.* [50], [51], [52], [53], [54], [55], [56] utilized a class activation heat-map algorithm named Grad-CAM, which uses gradient data for its calculations, and heat-maps to help in understanding the working of a deep model. They selected a transfer learning approach for training a deep model and modified the VGG16 by adding an extra dense layer at the end of the model. The model's performance is enhanced by Fastai [51], [55], [56], [57], [58] using the grad-CAM to highlight the brain regions

on MRI samples that the previous model used, making predictions selected. SGD loss function in combination with Nesterov intensity [52], [56], [57], [58] further improved the classification results, and the model attained a test accuracy of 97.89%.

The proposed model differs from other recently proposed methods in two ways:

- Firstly, a few researchers have used data augmentation techniques to improve their results. In contrast, none of the reviewed research papers regarding the classification of Alzheimer's disease has recognized the central problem of data-set imbalance. Our proposed model is oversampling the dataset by generating synthetic samples using SMOTETOMEK.
- Secondly, the previous models are trained using transfer learning containing many parameters affecting the network's efficiency. In contrast, the proposed model is built from scratch to precisely classify the stages of AD by decreasing parameters and calculation costs.

In DL, there is always scope for improvement, and most researchers have not achieved remarkable classification performance. Their methodologies and approaches suffer from various hindering factors because they have overlooked some inherent hurdles of DL models and medical image dataset [5], [12], [23]. The data set used in this research is collected from Kaggle, which contains 6400 samples of anonymous patients with only MRI scan images and their respective class labels information. It is a multi-class dataset consisting of four different classes, including a customary (NOD) class and three other classes representing three different early stages of AD, namely, Very Mild Demented (VMD), Mild Demented (MD), and Moderate Demented (MOD). It is a two-year-old data set, and various researchers have offered their contributions in this duration while obtaining good results by employing several techniques and combinations.

### III. THE PROPOSED ADD-NET MODEL FOR EARLY ALZHEIMER DIAGNOSIS

In the medicine and healthcare field, image processing has brought quite a revolution. Nowadays, image processing has applications in almost every aspect of the medical field. Doctors can examine the organs of the human body from the inside without the need for surgery during the diagnosis stage. There are various types of scans in the medical field: X-Ray, Ultrasound, Magnetic Resonance Imaging (MRI), and Computed Tomography (CT) scans. A human being cannot possibly examine medical scans as precisely as a machine is capable and draw accurate conclusions from them. A device trained on a medical image data set can provide accurate results within seconds, whereas, on the other hand, it might take a whole panel of doctors to derive the same conclusion in days. Modern health care systems depend upon computer vision and image processing algorithms as their integral part. The importance cannot be overstated. AD is becoming one of the most rapidly increasing diseases

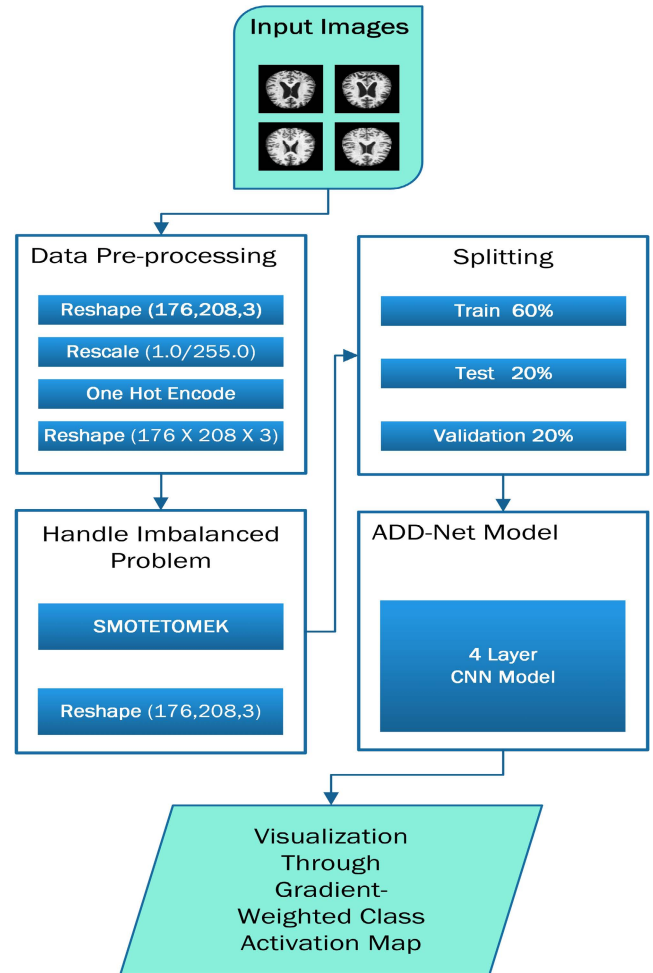


FIGURE 1. Methodology of the proposed ADD-Net for early detection of AD.

globally. A few researchers have used data augmentation techniques to improve their results. In contrast, none of the reviewed research papers regarding the classification of Alzheimer's disease has recognized the imbalance data-set issue. Some researchers failed to obtain notable results because they did not train their models enough. It is observed that research papers focus on discovering new approaches toward classification purposes for biomedical diagnoses. In this proposed model, the input data set is pre-processed using normalization. The essential process of converting the categorical data variables is to be provided to the ADD-Net using the one-hot encoder. Then, the Synthetic Minority Oversampling Technique (SMOTETOMEK) algorithm is utilized to solve the imbalanced data-set issue that over-samples the classes to balance the data-set. Afterward, the data set is split into train, test, and validation by 60%, 20%, and 20%, respectively. Furthermore, the features are extracted using a standard CNN for effectively training the ADD-Net, as shown in Fig. 1. The size of training parameters is smaller in comparison with [29], [31], and [33] for the robustness of the model in AD classification. The Grad-CAM heat-map algorithm is

utilized to visualize the class activation map, highlighting the features that lead to the classification of an image sample.

### A. DESCRIPTION OF THE AD DATASET

Several data sets are available on the internet for AD classification. Many AD data sets are in CSV format and are unsuitable for this research. Dedicated organizations like ADNI and OASIS also provide access to their data sets for research and educational purposes. However, the samples in both of these data sets are in 3-Dimensional image format, and the size of the data sets is gigantic. The OASIS data set is 18 gigabytes, while the ADNI dataset is 450 gigabytes. The data set used in this research is collected from Kaggle, which contains samples of anonymous patients with only MRI scan images and their respective class label information. It is a multi-class data set consisting of different views and four classes, including an average NOD class and three other classes representing three different early stages of AD. VMD, MD, and MOD are slightly observable with the bare eye in Fig. 2.

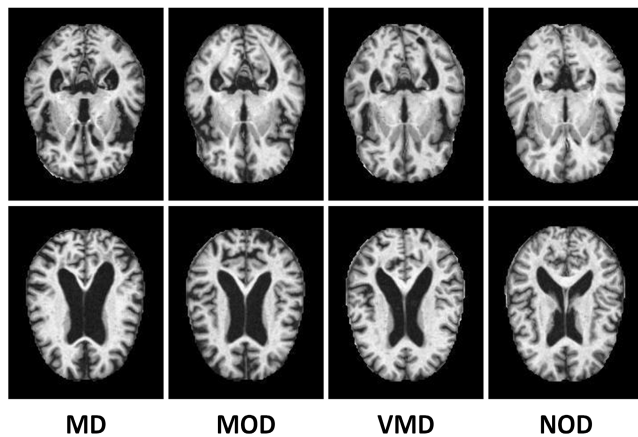


**FIGURE 2.** Image samples from AD dataset without up-sampling through SMOTETOMEK.

According to the description of the data set, each sample in the data set available on Kaggle is personally verified by the uploader himself. Also, the data set size is reasonable, and the pieces are already cleaned up, i.e., resized and organized. Based on these factors, this data set is used in our research. The data set has 6400 samples in total. The samples are individual three-channel (RGB) images of 176 x 208 pixels belonging to four different classes. The number of samples in the NOD class is 3200. The remaining three classes, VMD, MD, and MOD, have 2240, 896, and 64 images, respectively. The only downside of this data set is that it is imbalanced, as discussed in Table 2. To solve this problem, we use SMOTETOMEK to generate synthetic data for each imbalance class concerning the balanced class, as shown in Fig. 2. The data set is divided into 60%, 20%, and 20% for training, validation, and test set, respectively.

**TABLE 2.** AD data-set class distribution before up-sampling through SMOTETOMEK.

Class	No. of Images
Mild Demented (MD)	896
Moderate Demented (MOD)	64
Non-Demented (NOD)	3200
Very Mild Demented (VMD)	2240

### 1) BALANCING THE AD DATA SET USING SMOTETOMEK

Typically, oversampling and under-sampling are two techniques for re-sampling. However, another type of re-sampling approach exists, which is a hybrid of both methods. For this research study, we have employed the hybrid SMOTETOMEK algorithm. It combines SMOTE, the up-sampling algorithm, and TOMEK, the down-sampling method. SMOTE generates new samples relying on class nearest neighbors, while TOMEK is an implementation of condensed nearest neighbors. Both algorithms work in sequence, and SMOTE chooses a random instance from a minority class and increases its proportion by interpolating new samples. TOMEK then selects a random sample and discards it if its nearest neighbors belong to the minority class. In this way, SMOTETOMEK evens the examples of each type and effectively solves the dataset imbalance problem as depicted in Table 3. To balance out the data set, SMOTETOMEK utilizes the Nearest Neighbor technique to interpolate new imitation samples for the minority classes shown in Fig. 3.

**TABLE 3.** AD data-set class distribution after up-sampling through SMOTETOMEK.

Class	No. of Images
Mild Demented (MD)	3200
Moderate Demented (MOD)	3200
Non-Demented (NOD)	3200
Very Mild Demented (VMD)	3200

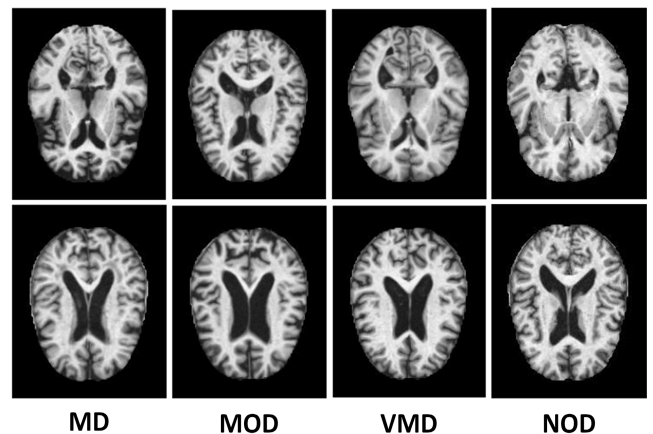


**FIGURE 3.** Synthetic image samples generated through SMOTETOMEK for all classes.

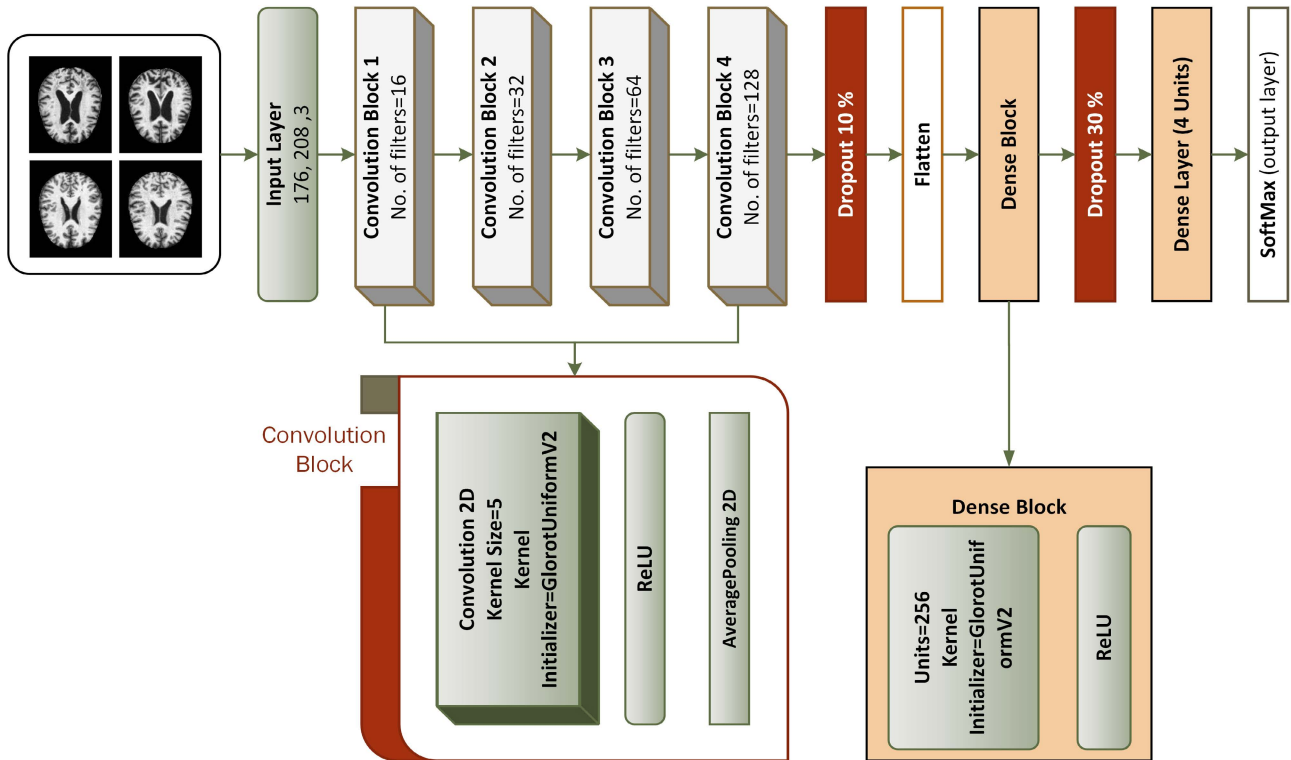


FIGURE 4. Architecture of the proposed ADD-Net for early detection of AD.

**B. ADD-NET MODEL COMPONENTS**

The main components of the proposed model are briefly discussed in the next subsections.

**1) THE PROPOSED ADD-NET NETWORK ARCHITECTURE**

The CNN architecture is based on the biological structure of the human brain, and it is mainly used in computer vision applications like image classification, image segmentation, and object detection. Previously designed deep models preferred it due to its translation-invariant nature [48]. The translation or space invariance implies that a CNN can recognize the same feature regardless of its position in various images. This paper proposes a novel CNN model from scratch to perform accurate AD classification. The proposed ADD-Net is comprised of four convolutional blocks, and each convolutional block has a Rectified Linear Unit (ReLU) activation function and a 2D average pooling layer, two dropout layers, two dense layers, and a SoftMax classification layer, as depicted in Fig. 4. The detailed network architecture and model summary of the proposed model used for the classification of AD with the subsequent layer is discussed in Table 4, and a description of hyper-parameters that plays a vital role in practical training of the ADD-Net model in Table 5.

**2) ADD-NET CONVOLUTIONAL BLOCKS**

The convolutional block is the main block of the proposed ADD-Net, and each convolutional block consists of

TABLE 4. Total parameters for the proposed ADD-Net model.

Model Summary		
Layer Type	Output Shape	Parameters
Input Layer	(None, 176, 208, 3)	0
ADD-NET Block01	(None, 86, 102, 16)	1216
ADD-NET Block02	(None, 41, 49, 32)	12832
ADD-NET Block03	(None, 18, 22, 64)	51264
ADD-NET Block04	(None, 7, 9, 128)	204928
Dropout_1	(None, 7, 9, 128)	0
Flatten	(None, 8064)	0
Dense_1	(None, 256)	2064640
Dropout_2	(None, 256)	0
Dense_2	(None, 4)	1028
Output: SOFTMAX	(None, 4)	0
Total Parameters		23,35,908
Trainable Parameters		23,35,909
Non-Trainable Parameters		0

a convolutional 2D, a ReLU, and an average-pooling2D. The kernel initializer is used to choose weights for the convolutional 2D layer. The ReLU activation function is used to overcome the gradient vanishing problem and allow the network to learn and perform faster. At the same time, the

TABLE 5. List of hyper parameters that are used in ADD-Net architecture.

Sr.#	Parameter Name	Parameter Type
1	Optimizer	SGD
2	Learning rate	0.01
3	Batch size	8
4	Epochs	40
5	Call back	ReduceLRonPlateau
6	Hidden layer activation	ReLU
7	Output layer activation	SoftMAX

convolutional 2D down-samples the image and its spatial dimensions by taking the average value over an input window (of size defined by pool\_size) for each channel of the input. The convolutional layers work in asymmetry, and the features are gradually built. Local patterns, like edges, lines, and curves, are extracted in the initial layers, and local features are extracted based on these patterns, as shown in Fig. 5. Consecutively, the model extracts high-level features and enables the deep model to classify an image more accurately.

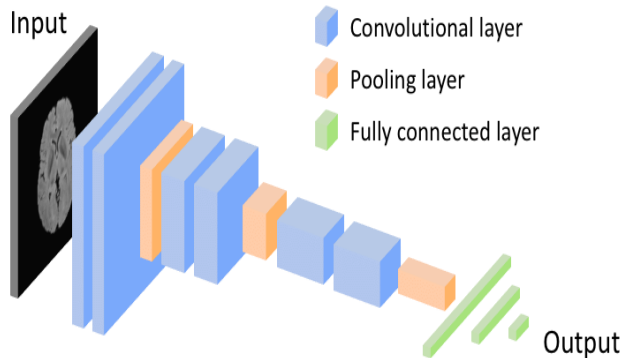


FIGURE 5. Typical CNN Model.

3) DROPOUT LAYER

Dropout layers turn nodes on and off to reduce the training time of the model and decrease the network complexity. Dropout randomly switches off nodes using probability distribution during each epoch, preventing models from over-fitting. As a result, the model learns all the relevant features and entirely contains various elements in each iteration.

4) FLATTEN LAYER

Flatten layer is placed between the convolution layers and dense layers. Convolution layers work with tensor data types for input, while dense layers require information in a 1-Dimensional format. Flatten layer vectorizes the feature map to feed it to dense layers, as depicted in Fig. 6.

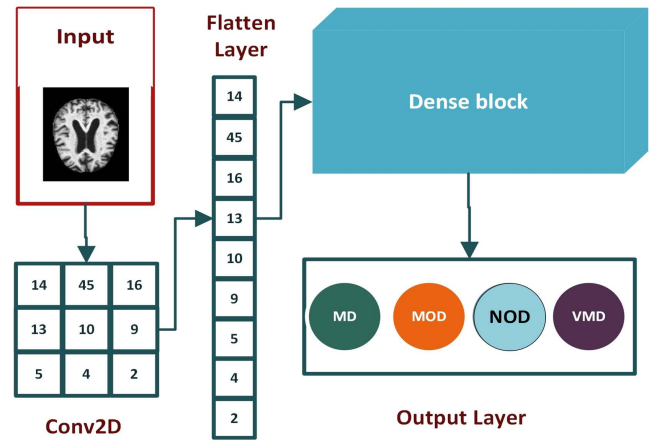


FIGURE 6. Details of flatten operation to vectorize the feature map.

C. DENSE BLOCK

There are two Dense blocks in the proposed architecture and each ADD-Net block has few layers. The details of each layer is discussed in the next subsection.

1) ReLU ACTIVATION

Activation functions are mathematical operations that decide whether output from a perceptron is to be forwarded to the next layer. In short, they activate and deactivate nodes in a deep model. The activation function is used in the output layer to start the node, which returns its label, which is then assigned to the image processed through the model. There are several activation functions. We used ReLU in hidden layers because of its simple and time-saving calculation. SoftMax, a probability-based activation function, is used for the output layer because our model is for multi-class classification.

2) DENSE LAYER

The dense layer is also called the fully connected layer. This layer inputs a single vector and produces output based on its parameters. The images are identified and assigned a class label in these layers. The learning of the model takes place in fully connected layers via the back-propagation method. The number of trainable parameters of a model is determined based on the number of values used in each dense layer. SoftMax is used after a couple of layers, with the number of neurons equal to the number of classes [49]. The labels are one-hot encoding in multi-class classification, and only the positive type is present in the loss term.

IV. EVALUATION OF THE PROPOSED ADD-NET MODEL

The experiments were executed on a personal computer system equipped with two Intel Xeon 2687W v4 (3.0 GHz clock speed, 12 cores, and 24 threads) CPUs, 64 GB RAM, 5 GB (NVIDIA) P2000 GPU (Graphical Processing Unit). The model's evaluation was conducted using the test set that was created from splitting the data set before training the model.

Using several metrics ensures the robustness of a model from every angle. The combined understanding of these results determines the successful training of a model. For instance, if accuracy is very high, say above 90% does not necessarily mean that the model is excellent. Several other factors are involved, like loss, over-fitting, etc. We employed different metrics to benchmark the performance of our model. The following terms are extensively used when observing various metrics of a classifier and the source code will be publicly available at <https://github.com/shahidzikria/ADD-Net>.

#### A. ACCURACY

Accuracy is the measure of total correct predictions out of accurate predictions obtained using the following expressions:

$$Accuracy = \left( \frac{TP + TN}{TP + FN + FP + TN} \right) \quad (1)$$

where TP, TN, FN, and FP are True Positive, True Negative, False Negative, and False Positive values, respectively.

#### B. PRECISION

Precision is the ratio of correct positive predictions to total positive predictions, and it is calculated using the following equation:

$$Precision = \left( \frac{TP}{TP + FP} \right) \quad (2)$$

#### C. RECALL

The recall is also known as the sensitivity score or actual positive rate. It is the comparison of correct positive predictions to total actual correct positives. The recall is calculated using the following equation:

$$Recall = \left( \frac{TP}{TP + FN} \right) \quad (3)$$

#### D. F1-SCORE

Ideally, a value of 1.0 in precision and 1.0 in the recall is considered an ideal case for a classification model. F1-score is the harmonic mean of precision and recall. F1-score is unique in the sense that it plots its graph with a separate line for each class label. The F1-score is computed using the following equation:

$$F1 = \left( 2 * \frac{Precision * Recall}{Precision + Recall} \right) \quad (4)$$

#### E. RECEIVER OPERATING CHARACTERISTICS (ROC) CURVE

A ROC curve is a graphical way to illustrate the possible connection between sensitivity and specificity for every possible cut-off for a combination of tests. The ROC-curve graph is displayed with the help of 1-specificity (on the x-axis) and sensitivity (on the y-axis). While the 1-specificity is False Positive Rate and sensitivity is True Positive Rate can be

obtained through the following expressions:

$$TPR = \left( \frac{FP}{FP + FN} \right) \quad (5)$$

$$FPR = \left( \frac{FP}{FP + TN} \right) \quad (6)$$

#### F. CONFUSION MATRIX

A confusion matrix is used to assess and calculate different metrics of a classification model. It provides the division of numbers and all the predictions a model has made during the training or testing phase.

#### G. LOSS FUNCTION

Loss functions calculate the mathematical difference between the predicted value and the actual value. For this research, we have used a categorical cross-entropy algorithm for loss.

$$Loss = y - \bar{y} \quad (7)$$

$$L_{CE} = - \sum_{n=1}^k (L_i \log(p_i)) \quad (8)$$

where  $\mathbf{L}$  is the calculated loss of each class, and  $\mathbf{P}$  is the probability calculated by the SOFT function.

#### H. THE PROPOSED MODEL COMPARISON WITH RECENT MODELS USING ROC

ROC curve is used to analyze the performance of clinical tests and, more specifically, the accuracy of a classifier for binary or multi-classification. The Area Under Curve (AUC) in a ROC curve is used to measure the usefulness of the classifier, where greater the AUC generally means greater the usefulness of the classifier. We check the usefulness and accuracy of our proposed ADD-Net model using the ROC curve using AD data-set with and without SMOTETOMEK. The proposed ADD-Net is compared using the AD dataset's ROC curve with DenseNet169, InceptionResNet V2, and VGG19. The proposed ADD-Net, DenseNet169, InceptionResNet V2, and VGG19 achieved ROC values of 79.79%, 91.17%, 82.37%, 95.21%, respectively on imbalanced AD dataset as depicted in Fig. 7. After balancing the AD dataset with SMOTE-TOMEK, the proposed ADD-Net, DenseNet169, InceptionResNet V2, and VGG19 achieved AUC values of 97.99%, 94.92%, 94.75%, 97.01%, respectively as depicted in Fig. 8.

#### I. ADD-NET COMPARISON WITH OTHER MODELS USING EXTENSION OF ROC FOR MULTI CLASS

ROC curves are commonly used in binary classification to investigate a classifier's output. Binarizing the output is required to expand the ROC curve and ROC area to multi-class or multi-label classification. One ROC curve can be generated for each label; however, each element of the label indicator matrix can also be treated as a binary prediction (micro-averaging). The proposed ADD-Net is compared using the Extension of the ROC curve with DenseNet169,



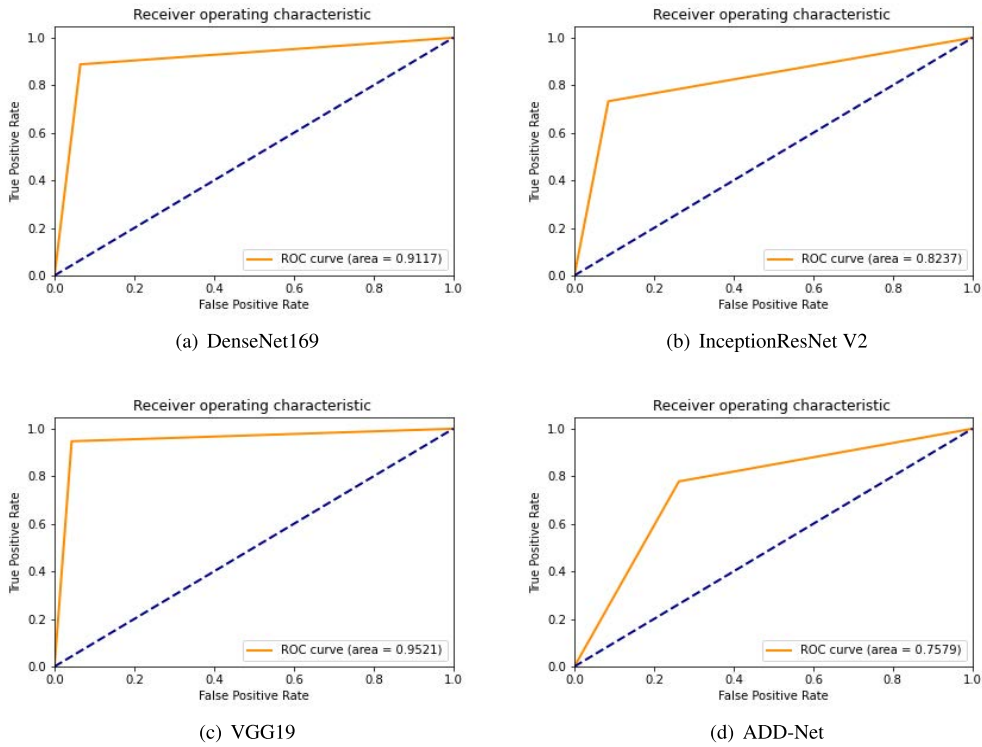


FIGURE 7. ROC curve results of DenseNet, InceptionResNet V2,VGG19 and ADD-Net without SMOTETOMEK.

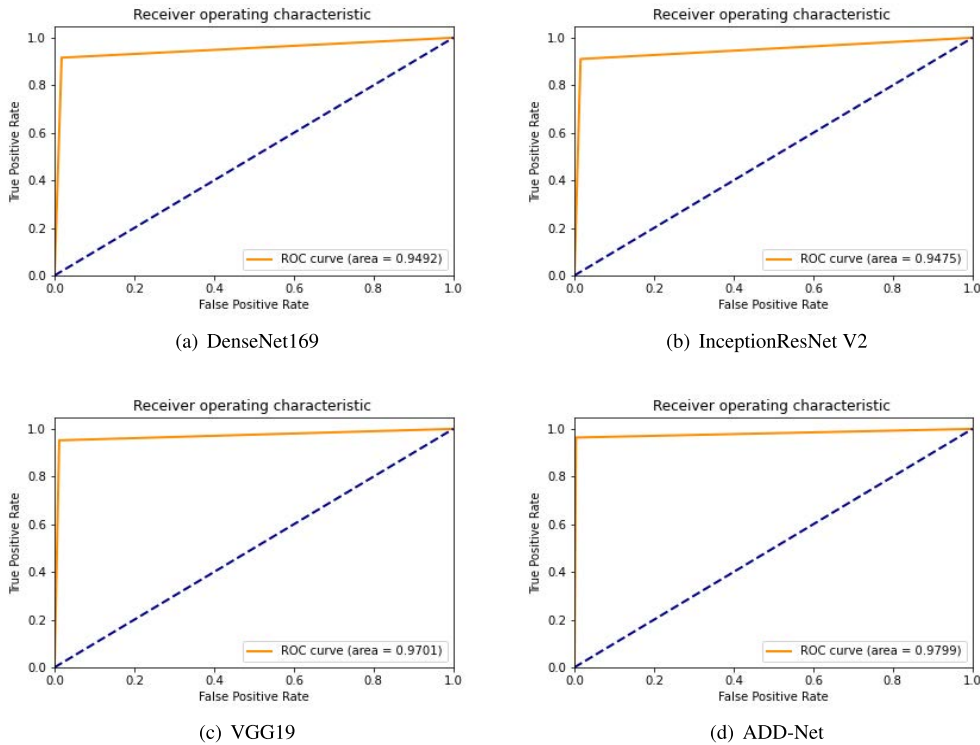


FIGURE 8. ROC curve results of DenseNet, InceptionResNet V2, VGG19 and ADD-Net with SMOTETOMEK.

InceptionResNet V2, and VGG19 on the balance and imbalance AD dataset as depicted in Fig. 9. We can note that after balancing the AD data-set using the SMOTETOMEK

algorithm, the AUC significantly for all the approaches, as shown in Fig. 10. AUC has also noted a similar effect for all the classes of the proposed ADD-Net. The AUC of

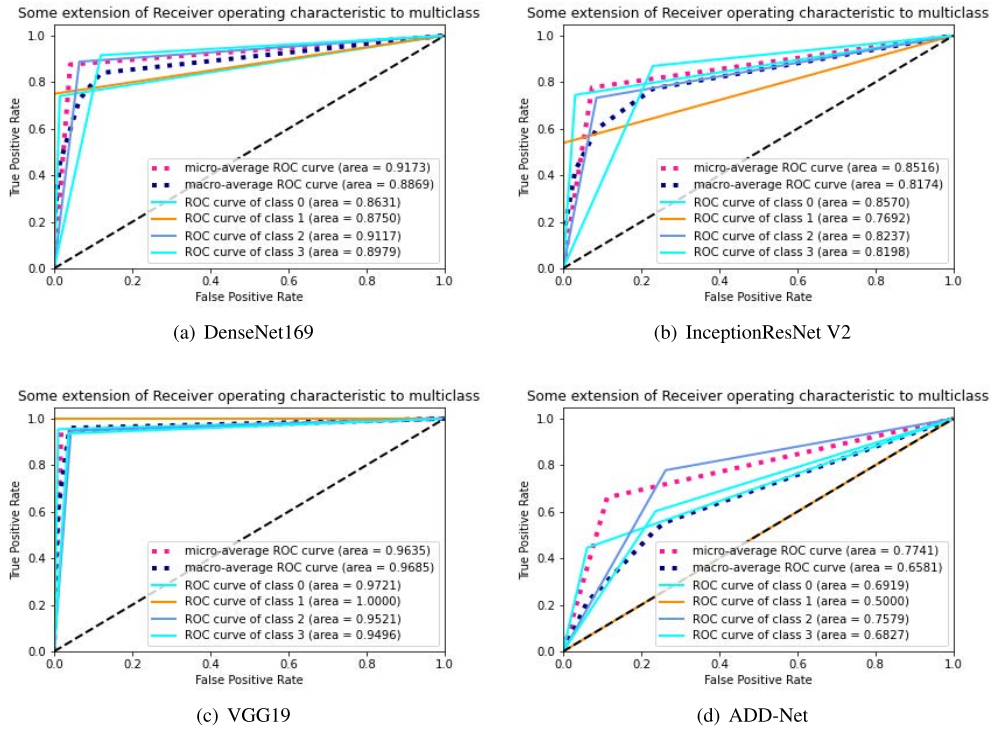


FIGURE 9. Extension receiver results of DenseNet, InceptionResNet V2, VGG19 and ADD-Net without SMOTETOMEK.

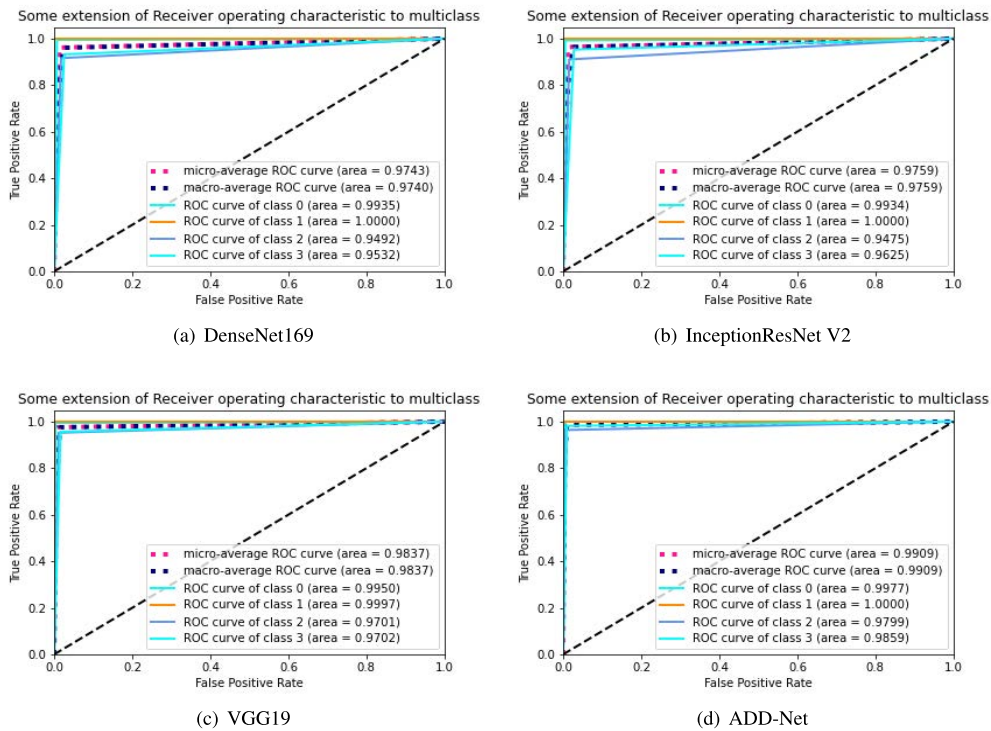
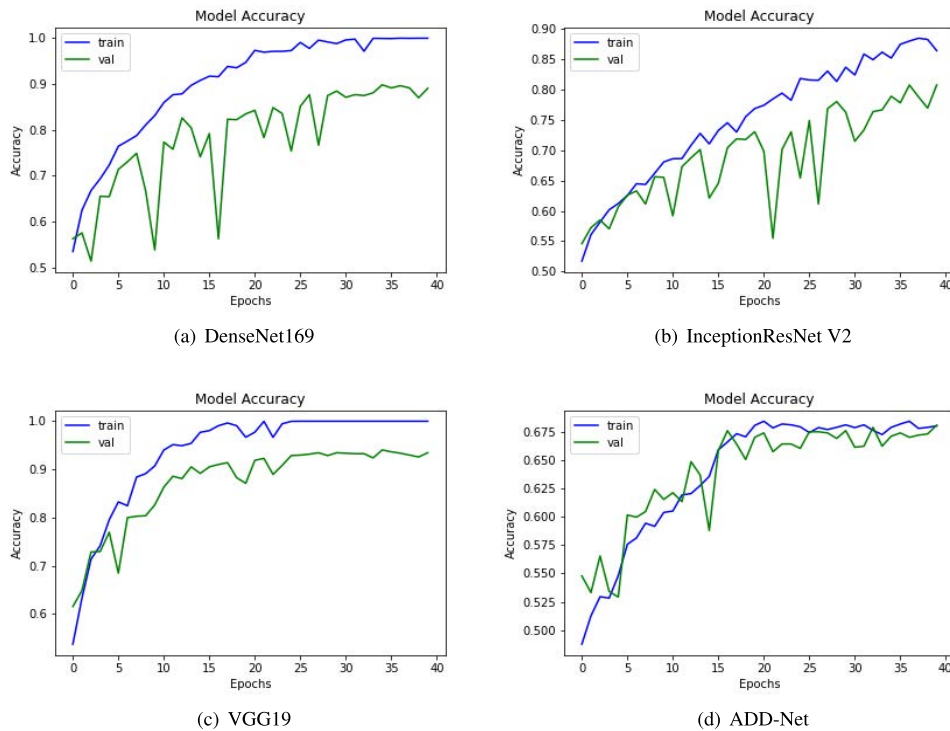


FIGURE 10. Extension receiver results of DenseNet, InceptionResNet V2, VGG19 and ADD-Net with SMOTETOMEK.

class 0 (MD), class 1 (MOD), class 2 (NOD), and class 3 (VMD) is 69.19%, 50.0%, 75.79%, and 68.27%, respectively without balancing the data-set. After balancing the AD

data-set, the AUC of class 0 (MD), class 1 (MOD), class 2 (NOD), and class 3 (VMD) is 99.7%, 1.00%, 98.10%, and 98.59%, respectively. These improvements in AUC prove the



**FIGURE 11.** Accuracy comparison of DenseNet169, InceptionResNet V2, VGG19 and ADD-Net without SMOTETOMEK.

authenticity of the SMOTETOMEK algorithm and feature selection of the ADD-Net model.

#### J. ACCURACY COMPARISON AGAINST OTHER MODEL WITH AND WITH SMOTETOMEK

SMOTETOMEK algorithm is applied to the data set to up-sample the number of images in classes with fewer samples. It increased the size of the data set from 6400 models to 12800 instances, i.e., 3200 equal numbers of pictures for each class. Hence, balancing out the data imbalance problem. The contrast between the two methods is utilizing the up-sampling technique, SMOTETOMEK.

The common point of both models is their architecture, consisting of a pre-trained model and fully connected dense layers for training. For a fair comparison, we evaluated our proposed and recent hybrid models like DenseNet169, VGG19, and InceptionResNet V2 using the same AD dataset before and after balancing it through SMOTETOMEK. The system provides remarkable results with SMOTETOMEK for the proposed and other models. The proposed ADD-Net model, DenseNet169, VGG19, and InceptionResNet V2 achieved an accuracy of 66.1%, 87.6%, 94.5%, 77.80%, respectively, using an imbalanced AD dataset as shown in Fig. 11. All models, like ADD-Net, DenseNet169, VGG19, and InceptionResNet V2, achieved accuracies of 98.63%, 96.14%, 97.56%, 96.03%, respectively, using the balanced AD data-set. This significant improvement in accuracies of all the models is visible from Fig. 12.

#### K. AUC COMPARISON OF PROPOSED MODELS WITH OTHER HYBRID MODELS

Several deep models were created to classify the early stages of AD. Some were conventional CNN models, while others were based on pre-trained deep architectures. Our proposed model is a deep CNN-based ADD-Net consisting of different ADD blocks and is very effective in classifying the different AD classes, as discussed earlier in this paper. We also created a few hybrid models using state-of-the-art classification models InceptionResNet V2, VGG19, and DenseNet169. The first model is a hybrid framework of DenseNet169 and MobileNet V2, reaching an AUC = 98% and AUC = 99% before and after balancing the AD data-set through SMOTETOMEK as depicted in Fig. 13. The second hybrid model was created using Inception ResNet V2 and MobileNet V2, and its evaluation AUC results are 94.8% and 99.6% AUC on balanced and imbalanced AD datasets, respectively. The third hybrid model is created through MobileNet V2 and VGG19, the AUC values for this model are 95.9% and 98.89% using balanced and imbalanced AD data sets, respectively. The proposed model attained AUC values of 99.89% and 98.99% on both AD datasets, as depicted in Fig. 14. As a result of the above discussion, we noted that the performance of the proposed model remains better and more consistent in comparison with hybrid models in the form of AUC.

#### L. LOSS COMPARISON OF ADD-NET WITH RECENT MODELS

Loss functions calculate the mathematical difference between predicted and actual values. For this research, we have used a

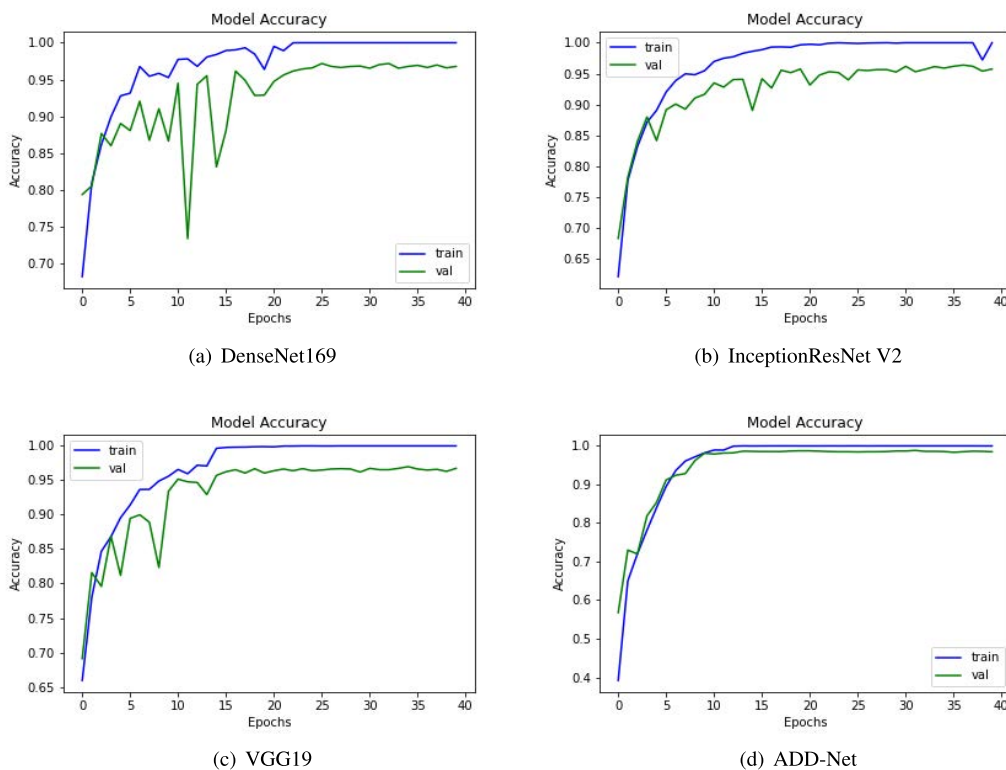


FIGURE 12. Training process Accuracy of DenseNet, InceptionResNet V2, VGG19 and ADD-Net with SMOTETOMEK.

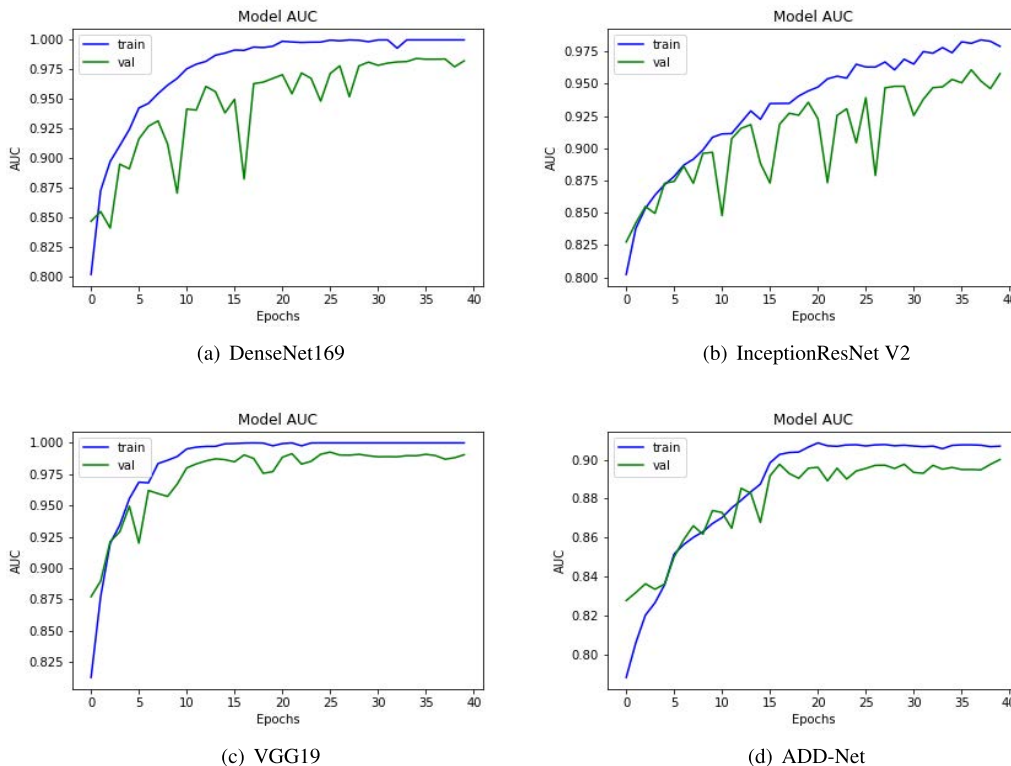
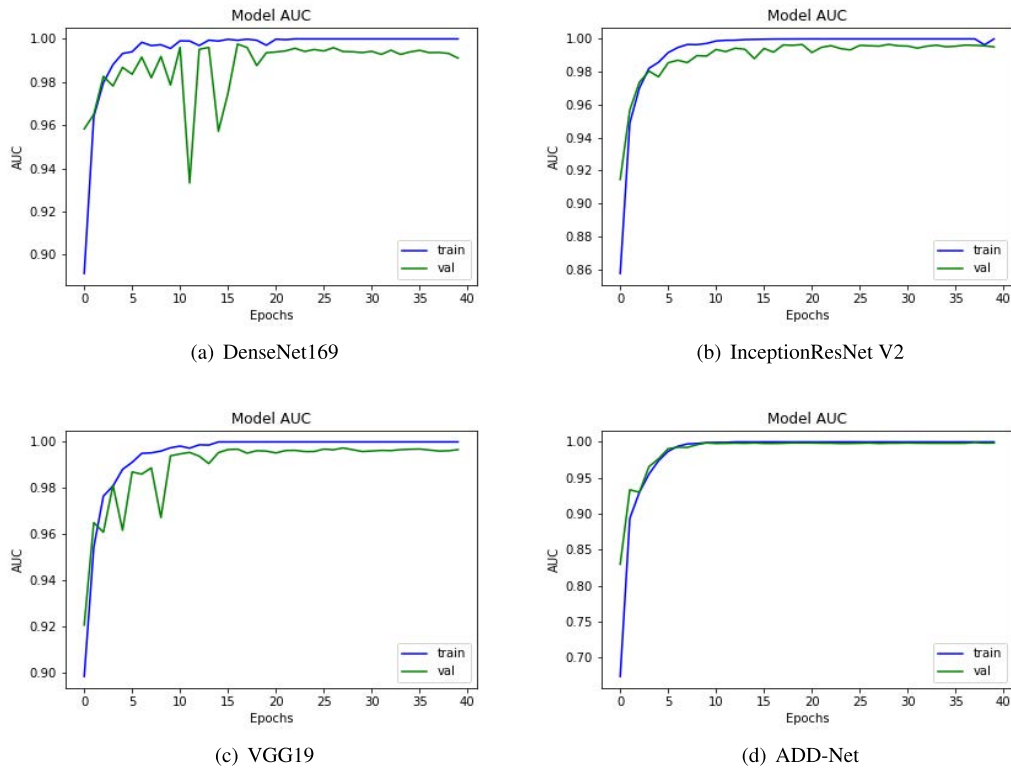


FIGURE 13. Training process AUC of DenseNet, InceptionResNet V2, VGG19 and ADD-Net without SMOTETOMEK.

categorical cross-entropy algorithm for loss calculation. Optimization functions are backtracking algorithms that adjust

the weights and biases of layers based on the value of the loss. However, the results are even more outstanding when



**FIGURE 14.** Training process AUC of DenseNet, InceptionResNet V2, VGG19 and ADD-Net with SMOTETOMEK.

the model is trained with up-sampled images. The proposed model's training accuracy reached 98.60%, while the validation obtained a 96.70% accuracy, 99.82% AUC, and an F1-score of 98.61%. The Loss values for InceptionResNet V2 are 0.1041 and 0.5364, DenseNet169 is 0.1595 and 0.3187, VGG19 is 0.2083 and 0.09, and ADD-Net is 0.05 and 0.76 on both the data sets with and without up-sampling through SMOTETOMEK as depicted in Figs. 15 and 16.

#### M. COMPARISON OF ADD-NET WITH RECENT MODELS USING F1-SCORE

The input data set is normalized in this suggested ADD-Net model. The fundamental procedure of converting categorical data variables is delivered to the model utilizing the one-hot encoder. The SMOTETOMEK technique is then used to correct the unbalanced data-set problem by oversampling the classes to balance the data set. We evaluated the ADD-Net model on the AD data set with recent models like DenseNet169, VGG19, and InceptionResNet V2 for a fair comparison. The system using SMOTETOMEK produces remarkable results for the suggested and other models. The proposed ADD-Net model, DenseNet169, VGG19, and InceptionResNet V2 achieved F1-score of 46.04%, 85.5%, 95.81%, 75.68%, respectively using an imbalanced AD data-set as shown in Fig. 17. All models, like ADD-Net, DenseNet169, VGG19, and InceptionResNet V2, achieved an F1-score of 98.6%, 96%, 97.50%, 96.1%, respectively, using the balanced

AD data-set. This significant improvement in accuracies of all the models is visible from Fig. 18.

#### N. COMPARISON OF ADD-NET WITH RECENT MODELS USING PRECISION

Several deep models were developed to classify Alzheimer's disease in its early stages. Some algorithms were traditional CNN, while others were pre-trained deep architectures. As mentioned earlier in this paper, our proposed model is a deep CNN-based ADD-Net comprising distinct ADD blocks. We compared our model with the InceptionResNet V2, VGG19, and DenseNet169 classification models as shown in Fig. 19; the first model is a hybrid framework of DenseNet169 and MobileNet V2 with precision values 88.7% 96.1% and before and after balancing the AD data-set using SMOTETOMEK. The second hybrid model was built with Inception ResNet-V2 and MobileNet V2, and its evaluation precision values are 79.9% 96.6% on balanced and unbalanced tasks, respectively. The third hybrid model is developed using MobileNet V2 and VGG19, with precision values are 94.7% and 97.6%, respectively, utilizing balanced and imbalanced AD data sets. As shown in Fig. 20, the proposed model achieved precision values are 74.5% 98.60% on both AD datasets. As a result of the preceding discussion, we discovered that the presented model's performance is better and more consistent than hybrid models in the form of precision.

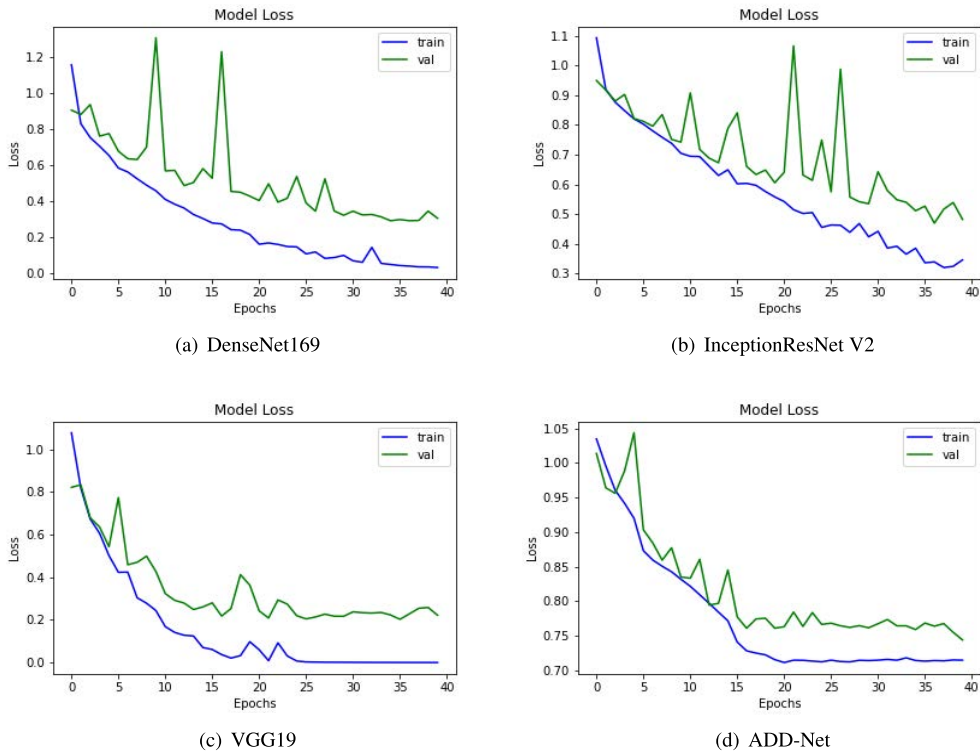


FIGURE 15. Training loss of DenseNet, InceptionResNet V2, VGG19 and ADD-Net without SMOTETOMEK.

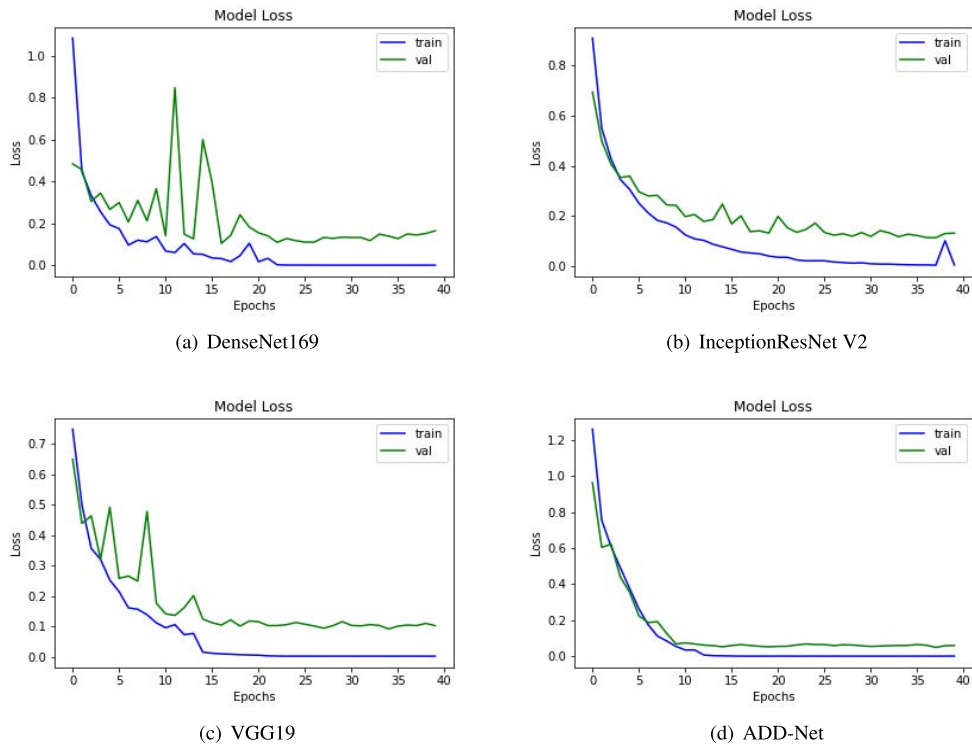


FIGURE 16. Training loss of DenseNet, InceptionResNet V2, VGG19 and ADD-Net with SMOTETOMEK.

**O. COMPARISON OF ADD-NET WITH RECENT MODELS USING CONFUSION MATRIX**

In this proposed ADD-Net model, the input data set is pre-processed using normalization. The essential process of

converting the categorical data variables is to be provided to the model using the one-hot encoder.

Then, the SMOTETOMEK algorithm is applied to resolve the imbalanced data-set issue that over-samples the classes

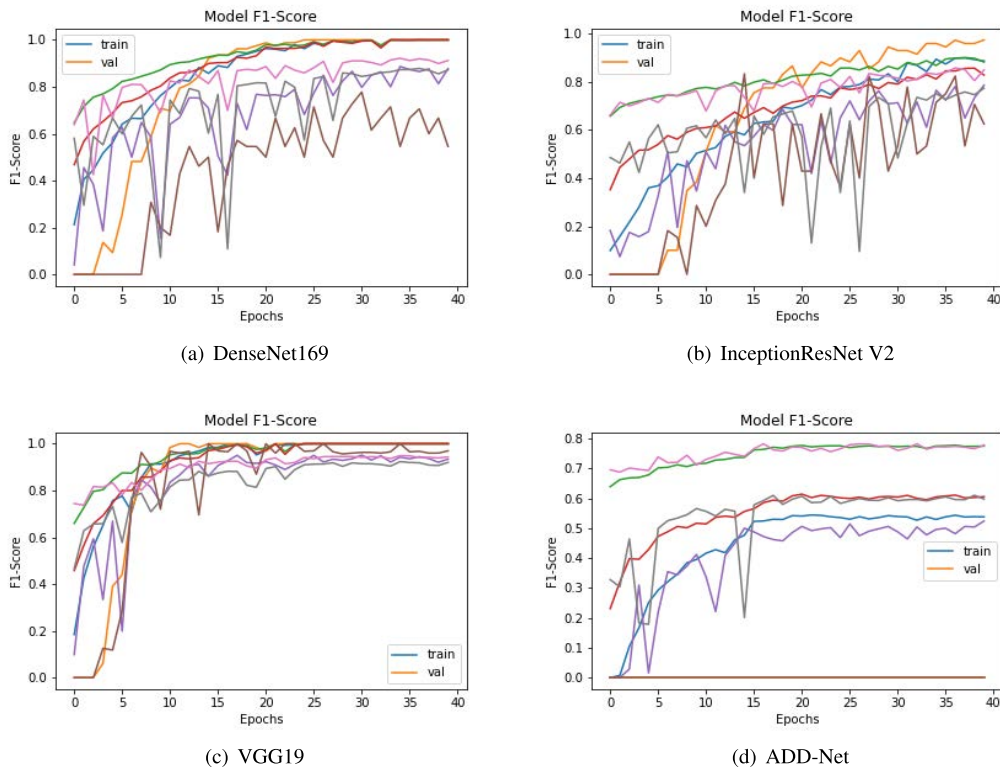


FIGURE 17. F1-Score of DenseNet, InceptionResNet V2, VGG19 and ADD-Net without SMOTETOMEK.

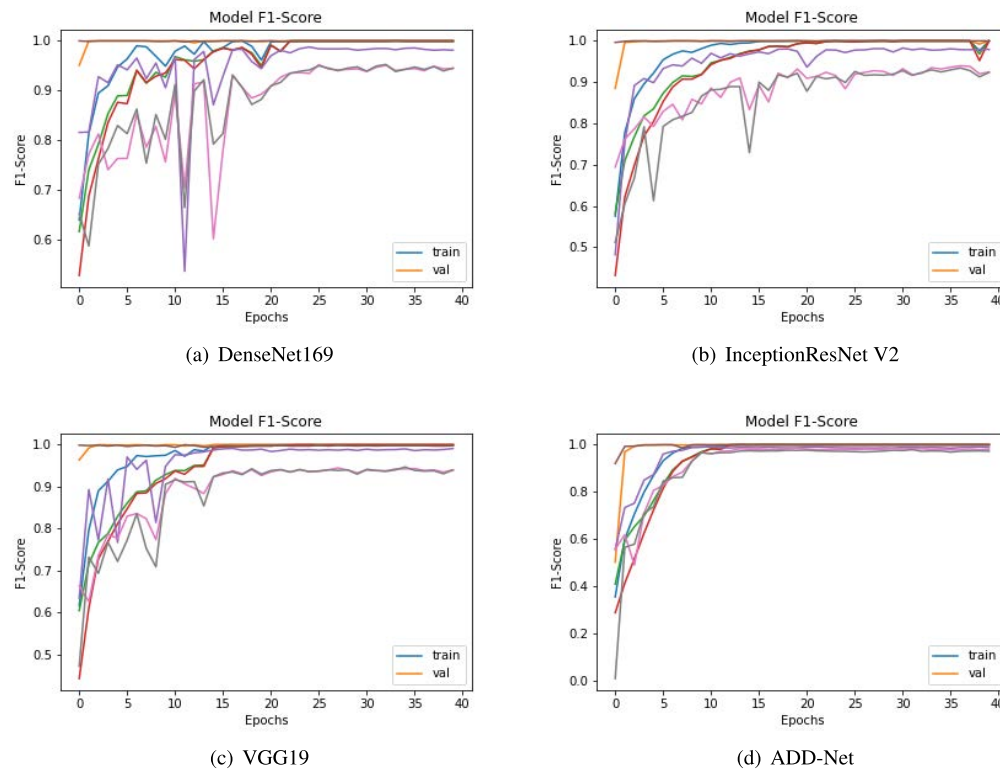


FIGURE 18. F1-Score of DenseNet, InceptionResNet V2, VGG19 and ADD-Net with SMOTETOMEK.

to balance the data-set. For a fair comparison, we assessed the ADD-Net model with recent models selected for

comparisons, like DenseNet169, VGG19, and Inception-ResNet V2 on the AD dataset before and after balancing

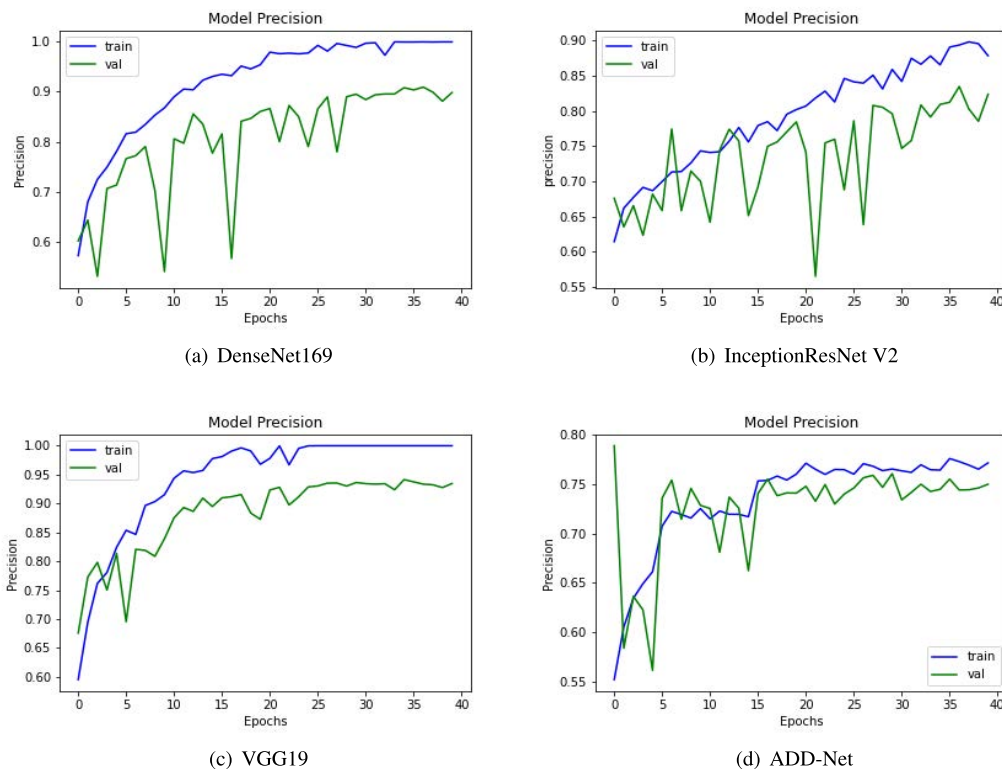


FIGURE 19. Precision results of DenseNet, InceptionResNet V2, VGG19 and ADD-Net without SMOTETOMEK.

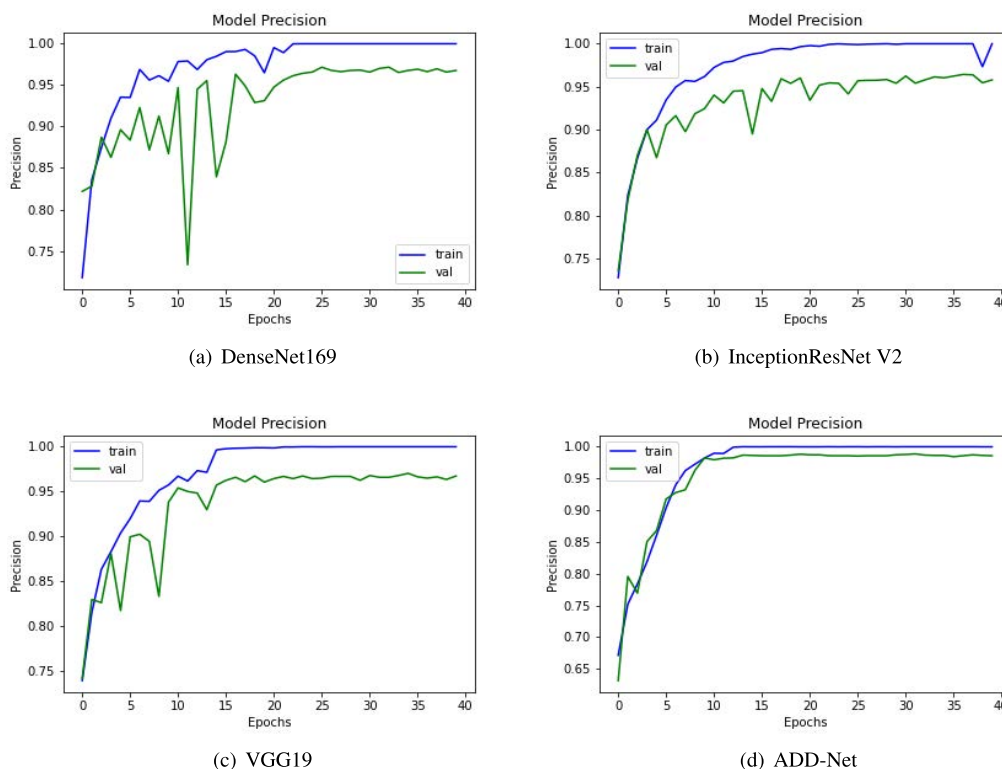


FIGURE 20. Precision results of DenseNet, InceptionResNet V2, VGG19 and ADD-Net with SMOTETOMEK.

it through SMOTETOMEK up-sampling algorithm. The system provides remarkable results with SMOTETOMEK

for the proposed and other models, as depicted in Figs. 21 and 22.



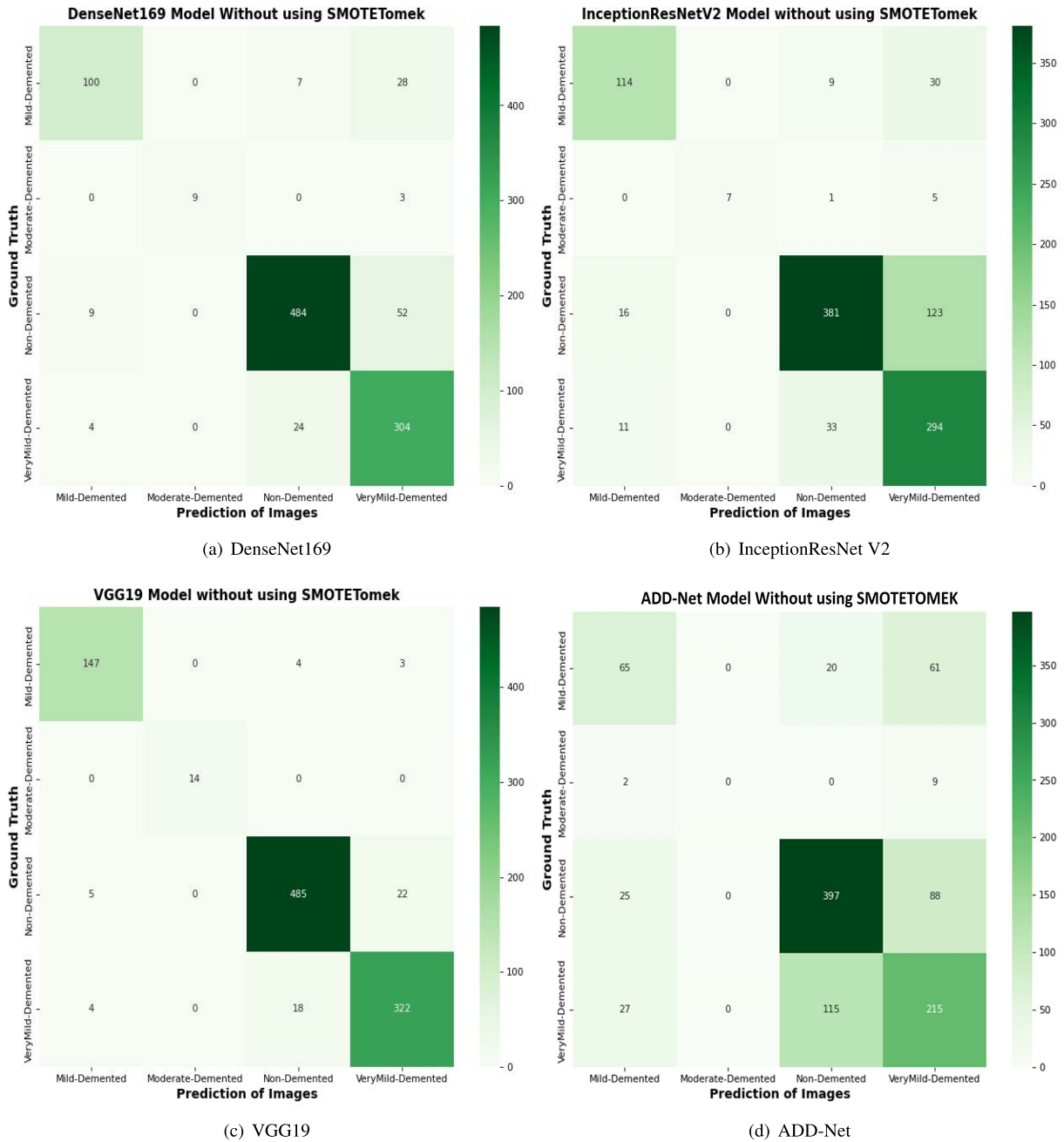


FIGURE 21. Confusion matrix’s of state-of-the-art algorithms and ADD-Net model without using SMOTETOMEK.

**P. VISUALIZATION THROUGH GRADIENT-WEIGHTED CLASS ACTIVATION MAP**

Grad-CAM detects the discriminatory regions for a CNN classification by calculating its CAM using gradient data. Grad-CAM visualizes a map of all the working classes by integrating gradient information. Grad-CAM considers 2D activation’s along with the average gradient information. It supports recognizing what a network perceives and which neuron is firing in a specific deep layer [48]. The preceding class gradient is related to the channel, ensuring the last CNN

layer generates a localization CAM displaying the image’s critical locations that substantially affect the deep model’s prediction, as shown in Fig. 23. To generate the CAM, the class gradient score is computed relative to the feature maps of the CNN layers [48].

**Q. DISCUSSION AND COMPARISON WITH OTHERS DEEP MODELS USING UP-SAMPLING**

The previous models used for comparison in this paper are not very effective in handling data imbalance problems

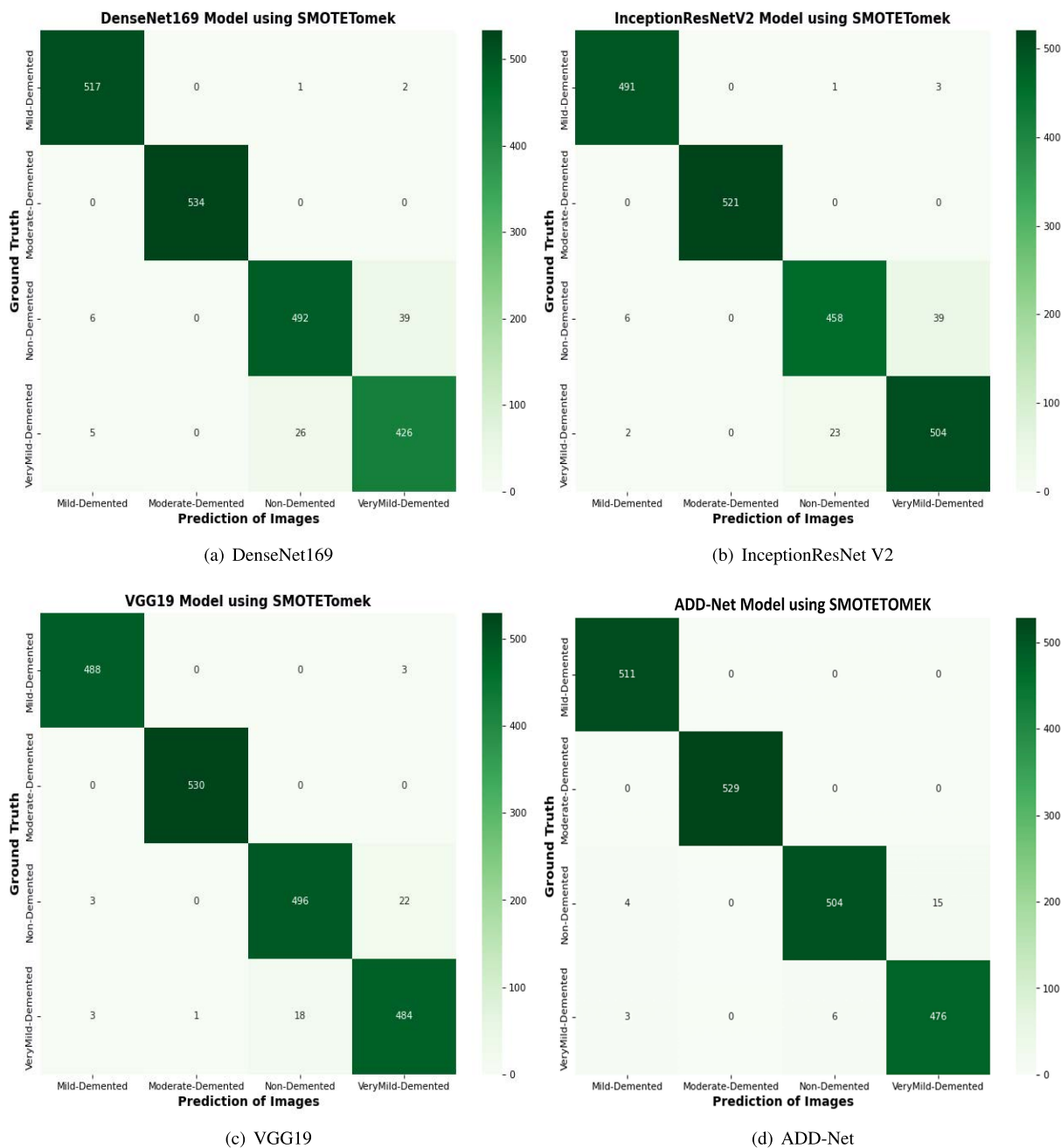


FIGURE 22. Confusion matrix's of state-of-the-art algorithms and ADD-Net model with using SMOTETOMEK.

and are limited in their performance. Sometimes suffer from over-fitting because of this data imbalance issue or lose their accuracy in correctly detecting the AD classes. The ADD-NET achieved maximum accuracy by using the SMOTETOMEK. However, the DEMENET attained an accuracy of 92.88% using the SMOTE algorithm. The proposed model performed with distinction among all the deep CNN, deep transfer learning, and hybrid models that we used for comparison in this research study. All the simulation results using different quality metrics are evidence of the performance of deep ADD-NET. The detailed comparison

of ADD-Net and other deep models with SMOTETOMEK is discussed in Table 6.

### V. LIMITATIONS

A solution to solve any real-world problem is not perfect in every aspect; this ideal case for a solution is used to solve a critical real-world problem that is well matured in its early versions and does not need upgrades. Solutions are prepared after studying the base requirement necessary to fix a problem and then gradually improve by analyzing real-time reviews about the system. In this proposed study, we present

**TABLE 6.** Performance comparison of ADD-Net with state-of-the-art algorithms.

Reference	Dataset	Accuracy	AUC	Precision	Recall	F1-score
Proposed ADD-Net (with SMOTETOMEK)	Kaggle	97.05%	99.89%	97%	97%	97.05%
Proposed ADD-Net (without SMOTETOMEK)	Kaggle	92.88%	98.99%	82%	89%	84.55%
DEMNET (with SMOTE)	Kaggle	95.23%	97%	96%	95%	95%
DEMNET (without SMOTE)	Kaggle	85%	92%	80%	88%	83%
Conv-BLSTM (SMOTE)	ADNI	82%	91%	78%	88%	82%
Conv-BLSTM (GAIN)	ADNI	82%	90%	79%	82%	82%
VGG16	ADNI	95.73%	-	96.33%	96%	95%
AlexNet	Kaggle	92.20%	99.45%	-	94.50%	-
ResNet-50	Kaggle	93.10%	98.82%	-	92.25%	-
Inception ResNet v2	Kaggle	79.12%	81.90%	70.64%	28.22%	39.91%

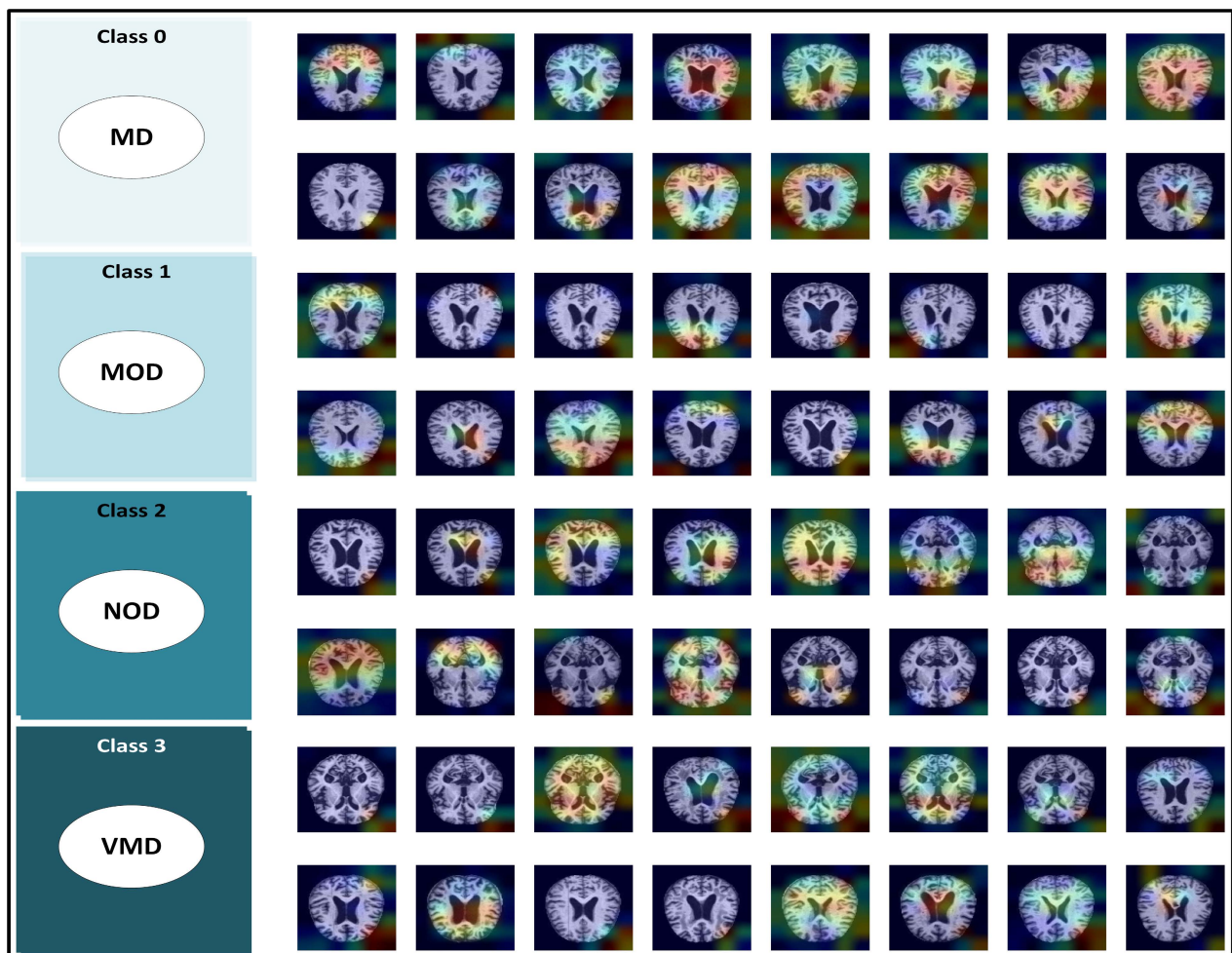


**FIGURE 23.** Generalization of the class activation map to locate the discriminative region through Grad-CAM.

a deep learning-based classification model named “ADD-Net” for classifying the early stages of Alzheimer’s disease.

Although outperforming other models still has shortcomings, the proposed model efficiency suffers on the imbalanced

dataset. As discussed above, due to an imbalanced dataset, the accuracy of deep learning models is compromised; our model suffers from the same problem when the dataset has a different number of samples in each class.

## VI. CONCLUSION

In this paper, we proposed a novel deep CNN for detecting AD with relatively few parameters, and the proposed solution is ideal for training a smaller dataset. The proposed Alzheimer's Disease Detection Network (ADD-Net) is built from scratch to precisely classify the stages of AD by decreasing parameters and calculation costs. Each block is specifically designed with many layers named ADD-block, which is used to classify the AD in its early stages for all the specific classes. The SMOTETOMEK method is employed for handling data-set imbalance problems for generating new instances to balance the number of samples for each category. Grad-CAM algorithm provides insight into CNN layers' working by visualizing class activation heat-map. Our proposed deep model provides outstanding accuracy of 96.70%, 97% precision, Sensitivity (Recall) of 97%, and an impressive AUC value of 99.82%. We will involve other pre-trained architectures and fine-tune transfer learning models to achieve more desirable results in the future.

## REFERENCES

- [1] A. Thaver and A. Ahmad, "Economic perspective of dementia care in Pakistan," *Neurology*, vol. 90, no. 11, pp. e993–e994, Mar. 2018.
- [2] P. Serge, V. Miquel, and J. Vernice, "Neurodegeneration: What is it and where are we," *J. Clin. Invest.*, vol. 111, no. 1, p. 3A10, 2003.
- [3] A. M. Sanford, "Mild cognitive impairment," *Clinics geriatric Med.*, vol. 33, no. 3, pp. 325–337, 2017.
- [4] A. B. Tufail, Y.-K. Ma, and Q.-N. Zhang, "Binary classification of Alzheimer's disease using sMRI imaging modality and deep learning," *J. Digit. Imag.*, vol. 33, no. 5, pp. 1073–1090, Oct. 2020.
- [5] K. Doi, "Computer-aided diagnosis in medical imaging: Historical review, current status and future potential," *Comput. Med. Imag. Graph.*, vol. 31, pp. 198–211, Jun. 2007.
- [6] S. Tiwari, V. Atluri, A. Kaushik, A. Yndart, and M. Nair, "Alzheimer's disease: Pathogenesis, diagnostics, and therapeutics," *Int. J. Nanomed.*, vol. 14, p. 5541, Jul. 2019.
- [7] C. Duyckaerts, B. Delatour, and M.-C. Potier, "Classification and basic pathology of Alzheimer disease," *Acta Neuropathologica*, vol. 118, no. 1, pp. 5–36, Jul. 2009.
- [8] L. G. Apostolova, A. E. Green, S. Babakhanian, K. S. Hwang, Y. Y. Chou, A. W. Toga, and P. M. Thompson, "Hippocampal atrophy and ventricular enlargement in normal aging, mild cognitive impairment and Alzheimer's disease," *Alzheimer Disease Associated Disorders*, vol. 26, no. 1, p. 17, 2012.
- [9] J. C. de la Torre, "Alzheimer's disease is incurable but preventable," *J. Alzheimer's Disease*, vol. 20, no. 3, pp. 861–870, May 2010.
- [10] D. A. Casey, D. Antimisiaris, and J. O'Brien, "Drugs for Alzheimer's disease: Are they effective?" *Pharmacy Therapeutics*, vol. 35, no. 4, p. 208, 2010.
- [11] M. Prince, "Dementia U.K.: Overview," Tech. Rep., 2014.
- [12] E. Nichols and T. Vos, "The estimation of the global prevalence of dementia from 1990–2019 and forecasted prevalence through 2050: An analysis for the global burden of disease (GBD) study 2019," *Alzheimer's Dementia*, vol. 17, no. S10, pp. e105–e125, Dec. 2021.
- [13] M. Tanveer, B. Richhariya, R. U. Khan, A. H. Rashid, P. Khanna, M. Prasad, and T. C. Lin, "Machine learning techniques for the diagnosis of Alzheimer's disease: A review," *ACM Trans. Multimedia Comput. Commun. Appl.*, vol. 16, no. 1s, pp. 1–35, Apr. 2020.
- [14] M. A. Ebrahimighahnavieh, S. Luo, and R. Chiong, "Deep learning to detect Alzheimer's disease from neuroimaging: A systematic literature review," *Comput. Methods Programs Biomed.*, vol. 187, Apr. 2020, Art. no. 105242.
- [15] J. Zhuang, J. Cai, R. Wang, J. Zhang, and W.-S. Zheng, "Deep kNN for medical image classification," in *Proc. Int. Conf. Med. Image Comput. Comput.-Assist. Intervent.* Cham, Switzerland: Springer, 2020, pp. 127–136.
- [16] R. Suganthe, M. Geetha, G. Sreekanth, K. Gowtham, S. Deepakkumar, and R. Elango, "Multiclass classification of Alzheimer's disease using hybrid deep convolutional neural network," *Nveo-Natural Volatiles Essential Oils J.*, vol. 8, pp. 145–153, Nov. 2021.
- [17] X. Jiang, L. Chang, and Y.-D. Zhang, "Classification of Alzheimer's disease via eight-layer convolutional neural network with batch normalization and dropout techniques," *J. Med. Imag. Health Informat.*, vol. 10, no. 5, pp. 1040–1048, May 2020.
- [18] P. Kalavathi and V. S. Prasath, "Methods on skull stripping of MRI head scan images—A review," *J. Digit. Imag.*, vol. 29, no. 3, pp. 365–379, 2016.
- [19] S. Basheera and M. S. S. Ram, "A novel CNN based Alzheimer's disease classification using hybrid enhanced ICA segmented gray matter of MRI," *Computerized Med. Imag. Graph.*, vol. 81, Apr. 2020, Art. no. 101713.
- [20] M. K. Singh and K. K. Singh, "A review of publicly available automatic brain segmentation methodologies, machine learning models, recent advancements, and their comparison," *Ann. Neurosci.*, vol. 28, nos. 1–2, pp. 82–93, Jan. 2021.
- [21] J. V. Manjón and P. Coupé, "Volbrain: An online MRI brain volumetry system," *Frontiers Neuroinform.*, vol. 10, p. 30, Jul. 2016.
- [22] B.-Y. Park, K. Byeon, and H. Park, "FuNP (fusion of neuroimaging preprocessing) pipelines: A fully automated preprocessing software for functional magnetic resonance imaging," *Frontiers Neuroinform.*, vol. 13, p. 5, Feb. 2019.
- [23] M. D. Zeiler and R. Fergus, "Visualizing and understanding convolutional networks," in *Proc. Eur. Conf. Comput. Vis.* Cham, Switzerland: Springer, 2014, pp. 818–833.
- [24] R. R. Selvaraju, M. Cogswell, A. Das, R. Vedantam, D. Parikh, and D. Batra, "Grad-CAM: Visual explanations from deep networks via gradient-based localization," in *Proc. IEEE Int. Conf. Comput. Vis. (ICCV)*, Oct. 2017, pp. 618–626.
- [25] L. Alzubaidi, M. A. Fadhel, O. Al-Shamma, J. Zhang, J. Santamaría, Y. Duan, and S. R. Olewi, "Towards a better understanding of transfer learning for medical imaging: A case study," *Appl. Sci.*, vol. 10, no. 13, p. 4523, Aug. 2020.
- [26] M. W. Weiner, D. P. Veitch, P. S. Aisen, L. A. Beckett, N. J. Cairns, R. C. Green, D. Harvey, C. R. Jack, W. Jagust, E. Liu, and J. C. Morris, "The Alzheimer's disease neuroimaging initiative: A review of papers published since its inception," *Alzheimer's Dementia*, vol. 9, no. 5, pp. e111–e194, Sep. 2013.
- [27] D. Marcus and T. Wang, "OASIS: Cross-sectional, MRI data in young, middle aged, nondemented, and demented, older adults," *J. Cogn. Neurosci.*, to be published.
- [28] J. Li, S. Fong, S. Mohammed, and J. Fiaidhi, "Improving the classification performance of biological imbalanced datasets by swarm optimization algorithms," *J. Supercomput.*, vol. 72, no. 10, pp. 3708–3728, 2016.
- [29] N. I. G. S. A. El-Aal, "A proposed recognition system for Alzheimer's disease based on deep learning and optimization algorithms," *J. Southwest Jiaotong Univ.*, vol. 56, no. 5, 2021.
- [30] B. A. Mohammed, E. M. Senan, T. H. Rassem, N. M. Makbol, A. A. Alanazi, Z. G. Al-Mekhlafi, T. S. Almurayziq, and F. A. Ghaleb, "Multi-method analysis of medical records and MRI images for early diagnosis of dementia and Alzheimer's disease based on deep learning and hybrid methods," *Electronics*, vol. 10, no. 22, p. 2860, Nov. 2021.
- [31] A. Pradhan, J. Gige, and M. Eliazer, "Detection of Alzheimer's disease (AD) in MRI images using deep learning," *Int. J. Eng. Res. Technol. (IJERT)*, vol. 10, pp. 580–585, Apr. 2021.
- [32] G. Vasukidevi, S. Ushasukhanya, and P. Mahalakshmi, "Efficient image classification for Alzheimer's disease prediction using capsule network," *Ann. Romanian Soc. Cell Biol.*, vol. 25, pp. 806–815, May 2021.
- [33] G. Battineni, N. Chintalapudi, F. Amenta, and E. Traini, "Deep learning type convolution neural network architecture for multiclass classification of Alzheimer's disease," in *Bioimaging*, 2021, pp. 209–215.

- [34] J. Islam and Y. Zhang, "Brain MRI analysis for Alzheimer's disease diagnosis using an ensemble system of deep convolutional neural networks," *Brain Informat.*, vol. 5, no. 2, pp. 1–14, 2018.
- [35] J. Islam and Y. Zhang, "An ensemble of deep convolutional neural networks for Alzheimer's disease detection and classification," 2017, *arXiv:1712.01675*.
- [36] J. Islam and Y. Zhang, "Early diagnosis of Alzheimer's disease: A neuroimaging study with deep learning architectures," in *Proc. IEEE/CVF Conf. Comput. Vis. Pattern Recognit. Workshops (CVPRW)*, Jun. 2018, pp. 1881–1883.
- [37] C. Szegedy, S. Ioffe, V. Vanhoucke, and A. A. Alemi, "Inception-v4, Inception-ResNet and the impact of residual connections on learning," in *Proc. 31st AAAI Conf. Artif. Intell.*, 2017, pp. 1–7.
- [38] S. H. Khan, M. Hayat, M. Bennamoun, F. A. Sohel, and R. Togneri, "Cost-sensitive learning of deep feature representations from imbalanced data," *IEEE Trans. Neural Netw. Learn. Syst.*, vol. 29, no. 8, pp. 3573–3587, Aug. 2017.
- [39] B. Xu, N. Wang, T. Chen, and M. Li, "Empirical evaluation of rectified activations in convolutional network," 2015, *arXiv:1505.00853*.
- [40] A. F. Agarap, "Deep learning using rectified linear units (ReLU)," 2018, *arXiv:1803.08375*.
- [41] M. M. Lau and K. H. Lim, "Review of adaptive activation function in deep neural network," in *Proc. IEEE-EMBS Conf. Biomed. Eng. Sci. (IECBES)*, Dec. 2018, pp. 686–690.
- [42] F. Chollet, "Xception: Deep learning with depthwise separable convolutions," in *Proc. IEEE Conf. Comput. Vis. Pattern Recognit.*, Jul. 2017, pp. 1251–1258.
- [43] A. G. Howard, M. Zhu, B. Chen, D. Kalenichenko, W. Wang, T. Weyand, M. Andreetto, and H. Adam, "MobileNets: Efficient convolutional neural networks for mobile vision applications," 2017, *arXiv:1704.04861*.
- [44] G. Huang, Z. Liu, L. Van Der Maaten, and K. Q. Weinberger, "Densely connected convolutional networks," in *Proc. IEEE Conf. Comput. Vis. Pattern Recognit. (CVPR)*, Jul. 2017, pp. 4700–4708.
- [45] T. Fushiki, "Estimation of prediction error by using K-fold cross-validation," *Statist. Comput.*, vol. 21, no. 2, pp. 137–146, Apr. 2011.
- [46] J. Huang and C. X. Ling, "Using AUC and accuracy in evaluating learning algorithms," *IEEE Trans. Knowl. Data Eng.*, vol. 17, no. 3, pp. 299–310, Mar. 2005.
- [47] N. C. Thompson, K. Greenewald, K. Lee, and G. F. Manso, "The computational limits of deep learning," 2020, *arXiv:2007.05558*.
- [48] F. Wen and A. K. David, "A genetic algorithm based method for bidding strategy coordination in energy and spinning reserve markets," *Artif. Intell. Eng.*, vol. 15, no. 1, pp. 71–79, Jan. 2001.
- [49] L. Wang, X. Wang, J. Fu, and L. Zhen, "A novel probability binary particle swarm optimization algorithm and its application," *J. Softw.*, vol. 3, no. 9, pp. 28–35, Dec. 2008.
- [50] M. Raju, M. Thirupalani, S. Vidhyabharathi, and S. Thilagavathi, "Deep learning based multilevel classification of Alzheimer's disease using MRI scans," in *IOP Conf. Ser., Mater. Sci. Eng.*, vol. 1084, no. 1, 2021, Art. no. 012017.
- [51] J. Howard and S. Gugger, "Fastai: A layered API for deep learning," *Information*, vol. 11, no. 2, p. 108, Feb. 2020.
- [52] T. Dozat. (2016). *Incorporating Nesterov Momentum into Adam*. Dostupnéz. [Online]. Available: [http://cs229.stanford.edu/proj2015/054\\_report.pdf](http://cs229.stanford.edu/proj2015/054_report.pdf)
- [53] E. Kauderer-Abrams, "Quantifying translation-invariance in convolutional neural networks," 2017, *arXiv:1801.01450*.
- [54] A. De and A. S. Chowdhury, "DTI based Alzheimer's disease classification with rank modulated fusion of CNNs and random forest," *Expert Syst. Appl.*, vol. 169, May 2021, Art. no. 114338.
- [55] N. V. Chawla, K. W. Bowyer, L. O. Hall, and W. P. Kegelmeyer, "SMOTE: Synthetic minority over-sampling technique," *J. Artif. Intell. Res.*, vol. 16, no. 1, pp. 321–357, Jan. 2002.
- [56] M. Odusami, R. Maskeliūnas, R. Damaševičius, and T. Krilavičius, "Analysis of features of Alzheimer's disease: Detection of early stage from functional brain changes in magnetic resonance images using a finetuned ResNet18 network," *Diagnostics*, vol. 11, no. 6, p. 1071, Jun. 2021.
- [57] A. M. Alhassan, "Enhanced fuzzy elephant herding optimization-based Otsu segmentation and deep learning for Alzheimer's disease diagnosis," *Mathematics*, vol. 10, no. 8, p. 1259, Apr. 2022.
- [58] M. Odusami, R. Maskeliūnas, and R. Damaševičius, "An intelligent system for early recognition of Alzheimer's disease using neuroimaging," *Sensors*, vol. 22, no. 3, p. 740, Jan. 2022.



**MIAN MUHAMMAD SADIQ FAREED** received the Ph.D. degree in computer science and technology from Xi'an Jiaotong University, Xi'an, China. He is currently working as an Associate Researcher with the Institute of Artificial Intelligence and Marine Robots, Dalian Maritime University, Dalian, China. Previously, he worked as an Assistant Professor at the Department of Computer Science, Khwaja Fareed University of Engineering and Information Technology. He also worked as an Associate Professor at the School of Information Science, Guilin University of Technology, Guilin, China. He has completed a Post doctoral Research Fellowship at the Computer Vision and Pattern Recognition Laboratory, School of Electronics and Information Engineering, Xi'an Jiaotong University. He has published more than 20 journals and international conferences. His research interests include analyzing dynamic visual data, including video analysis and visualizations of multi-view data. His research awards and honors include a four-year scholarship from Xi'an Jiaotong University as an Outstanding Ph.D. Student, the Best Ph.D. Student of the year 2015, and a Postdoctoral Fellowship. He is also working as an Academic Editor in the *Journal of Healthcare Engineering*.



**SHAHID ZIKRIA** received the bachelor's degree (Hons.) in computer science from the Khawaja Fareed University of Engineering and Information Technology, Rahim Yar Khan, in 2022. He is currently pursuing the master's degree in computer science with the Department of Computer Science, Information Technology University, Lahore, Pakistan. He is currently working as a Research Assistant with the KFUEIT Research Laboratory. He has experience working in medical images, especially MRI scans, CT scans, and X-ray scans. His research interests include image processing, deep learning, computer vision, artificial intelligence, and federated learning.



**GULNAZ AHMED** received the master's degree in computer science with a specialization in telecommunications and networking from Bahria University, Pakistan, in 2013, and the Ph.D. degree in 2017. She is currently an Associate Researcher with the Institute of Artificial Intelligence and Marine Robots, Dalian Maritime University, Dalian, China. Previously, she worked as an Assistant Professor at the Department of Computer Science, Khwaja Fareed University of Engineering and Information Technology. She achieved the highest CGPA in master's degree and was awarded the Gold Medal and a merit-based scholarship from Bahria University. In 2014, she was selected for the International Young Talent Scholarship by Xian Jiaotong University. In 2017, she achieved the Best Student of the Year Award for annual performance from the School of International Education, Xian Jiaotong University, China. She has been awarded the SAN QIAN Scholarship by the provincial government. She has completed many national-level and provincial-level projects during her Post doctoral Fellowship.



**MUI-ZZUD-DIN** was born in Multan, Pakistan, in 1980. He received the B.Sc., M.I.T., and M.S. degrees in computer science from Bahauddin Zakariya University, Multan, in 2001, 2005, and 2014, respectively. From 2007 to 2021, he worked as a Lecturer with different educational institutes. Since January 2022, he has been working as a Lecturer with the Department of Computer Science and IT, Ghazi University, Dera Ghazi Khan. He has almost 14 years of teaching experience. His current

research interests include image processing, computer vision, deep learning, and data science.



**SAQIB MAHMOOD** was born in Rahim Yar Khan, Pakistan. He received the master's degree (Hons.) from the Khawaja Fareed University of Engineering and Information Technology, in 2020. He is currently working as an Assistant Lecturer with the Department of Computer Science, Khawaja Fareed University of Engineering and Information Technology. From 2018 to 2020, he received a Distinction certificate (Gold Medalist) for his master's degree.

He has about five years of experience as a Teacher. His current research interests include image processing, computer vision, deep learning, federated learning, and data science.



**MUHAMMAD ASLAM** received the M.S. degree from the Department of Electrical Engineering (Networking), COMSATS University Islamabad, Islamabad, Pakistan, and the Ph.D. degree from the School of Computer Science and Technology, Dalian University of Technology, Dalian, China, in June 2018, under the supervision of Prof. Xiaopeng Hu. He is currently a Lecturer with the University of the West of Scotland. Before that, he was a Postdoctoral Research Scholar at the

School of Cyber Science and Engineering, Wuhan University, under the International Postdoctoral Exchange Fellowship Program. His research interests include machine learning, cyber security, software defined networking, wireless sensor networks, and networks security.

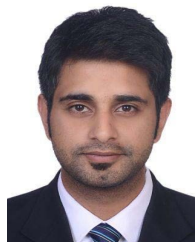


**SYEDA FIZZAH JILLANI** received the Ph.D. degree in antennas and electromagnetics from the Queen Mary University of London, U.K., in 2018. She is currently working as a Lecturer in radio spectrum engineering with the Department of Physics, Aberystwyth University, U.K. Before that, she worked as a Research Scientist at the University of Maine, USA, on a U.S. Department of Energy (DOE) Project on the technology transition of harsh-environment RF sensors to the industry, since February 2019.



**AHMAD MOUSTAFA** received the Ph.D. degree in computer science from the University of Wollongong, Australia. He was a Visiting Researcher at The University of Adelaide, the Auckland University of Technology, and Data61, Australia. He is currently an Associate Professor with the Nagoya Institute of Technology. His main research interests include federated learning, complex automated negotiation, multi-agent reinforcement learning, trust and reputation in multi-

agent societies, deep reinforcement learning, service-oriented computing, collective intelligence, intelligent transportation systems, and data mining. He is a member of the Japan Society for Artificial Intelligence, the IEEE Computer Society, the Australian Computer Society, and the Service Science Society of Australia.



**MUHAMMAD ASAD** (Student Member, IEEE) received the B.S. degree in telecommunication and networking from COMSATS University Islamabad, Wah Campus, Pakistan, in June 2014, and the M.S. degree in computer science from the Dalian University of Technology, Dalian, China, in June 2018. He is currently pursuing the Ph.D. degree in computer science with the Department of Computer Science, Nagoya Institute of Technology, Japan, under the supervision of Prof. Ahmed

Moustafa. His primary research interests include federated learning, deep learning, software-defined networking (SDN), wireless sensor networks (WSNs), and the Internet of Things (IoT). He was a recipient of the Chinese Government Scholarship (CSC), from 2015 to 2018. He also receives the Japanese Government Scholarship (MEXT) (2019–2023).

...